CHALMERS

Short-Slot Hybrid Coupler in Gap Waveguides at 38 GHz
Master of Science Thesis in Wireless and Photonics Engineering 2011

BILAL HUSSAIN

Chalmers University of Technology
Department of Signals and Systems
Göteborg, Sweden, June 2011

Short-Slot Hybrid Coupler in Gap Waveguides at 38 GHz

BILAL HUSSAIN

© BILAL HUSSAIN, June 2011.

Examiner: PER-SIMON KILDAL

Cover: Picture shows manufactured Short-Slot hybrid coupler, it was taken at antenna department in Chalmers University of Technology and is a property of the department.

I would like to dedicate my work to my parents. Their support and guidance always enlightened the path of success for me.

Acknowledgements

My heartiest gratitude to all those who supported me during this thesis work. I am really grateful to

- Prof, Per-Simon Kildal for his support and guidance throughout this thesis. He has provided me with the opportunity to work with him in the first place. Throughout this thesis work, he was always there whenever I needed. The knowledge that I possess in the field of microwave and antennas, has a huge contribution from him. Under his supervision I have learnt a lot and this experience will cherish my memories for the rest of my life.

- Mr. Ashraf Uz Zaman for being so nice and helpful throughout this project. He was always available to answer my questions. After discussing with him, I always found the problems solved in a simple and understandable way. A large portion of this thesis work is based on his ideas and research. I really regard and thank his efforts for making this possible.

- Mr. Tomas Ostling, without his support it was never possible. He always shared his R & D experience and guided me on the right path. I really appreciate his punctuality and humbleness. He was always an easy to talk person. I am really thankful to him.

- Dr, Jian Yang, for his support and theoretical knowledge he was delivered during the antennas course.

- Anders Edquist from ansoft support team, who has always provided me help with HFSS. I really owe him for his availability during the crucial stages of this thesis.

- Syed Hassan Raza, for being a nice office mate and also for clarifying my concepts.

- Syed Kashan Ali, for his moral support during hard times. He was always there to boast up my moral.

- Ali Imran Sandhu, for the knowledge he has provided me for HFSS at the very start of my thesis

- Engr, Ashiq Hussain, who not only supported me as a father but also inspired me to work harder. He was always there to guide me on the right course of action.

- The research group at antenna department and all the students of MPMPE. You all have contributed directly or indirectly. I am really thankful to you all for making my masters a life time experience.

Abstract

This thesis is an attempt to validate the recently developed gap waveguide technology. Gap waveguides are modified form of conventional microstrip and hollow waveguides. It provides two alternatives such as ridge gap waveguide and groove gap waveguide. This thesis mainly encapsulates the groove gap waveguides. Groove gap waveguides have similarities with hollow rectangular waveguides. This fact is used in this thesis by designing a short-slot hybrid coupler in groove gap waveguides, which is based on the techniques of rectangular waveguides. The hybrid coupler is designed in Q band with a 7.7% bandwidth.

In chapter 1, the need for this new technology is motivated by explaining the problems with traditional. Mechanical imperfections and strong electrical contact problems pose serious challenges to component design at high frequencies. Chapter 2 explains the comparison of different types of couplers with focus on short-slot hybrid coupler in rectangular waveguides. Chapter 3 mainly concerns the theoretical and analytical approach behind gap waveguides technology. It shows the required designing techniques and similarities with conventional technologies. Most of the text and figures are taken from the research papers published by Prof,Per-Simon Kildal and his colleagues. References are provided to the best of author's knowledge.

Chapter 4 uses the knowledge of chapter 2 & 3, and explains a procedure to design a 3dB coupler in groove gap waveguides at 38 GHz to meet those specifications that are valid for 3dB couplers in normal rectangular waveguide. The method for designing is explained in detail, also some other design variations are discussed at the end of this chapter. Chapter 5 explains the flexibility of groove gap waveguides by presenting a coupler of chapter 4 designed to interface with standard rectangular waveguides. It also shed some light on mechanical issues related to groove gap waveguide. Finally chapter 6 validates the results of chapter 4 & 5 by presenting the actual measurements performed on the device. It also establishes the fact that gap waveguide technology can be used for designing high frequency components with accuracy and flexibility. It also depicts that the

proposed design of early chapters actually possess a 9.1% bandwidth, which can be optimized to 10% easily.

Key Words: Short-slot Hybrid coupler, Gap waveguides, Groove Gap waveguides, Riblet Coupler

Contents

Table of Figures

Preface

This report is presented as a partial fulfillment for the degree of Master of Science in Wireless and Photonics engineering. The work was funded by Arkivator AB, which is a Swedish company specialized in high frequency passive components and was performed at signal and systems department, in Chalmers University of Technology. My examiner and main supervisor was Prof,Per-Simon Kildal. My co-supervisor was Mr, Ashraf Uz Zaman, who is a PhD student at Chalmers University of Technology. The industrial supervisor for this project was Mr, Tomas Ostling, who is R&D manager at Arkivator AB, Goteborg Sweden.

1 Chapter 1

1.1 Introduction:

Telecommunication is one of the fastest growing industries in today's global economy. The reason behind this tremendous growth is the development of cheap and reliable RF solutions. With the growth in RF applications, requirement for high data rates and bandwidth is also increasing. Moreover, as the hand held devices are common in use, requirement on size and battery usage is more stringent. This causes the need for a frequency shift in RF spectrum to manufacture devices in mm sizes. Another important application is emerging in the field of Terahertz. As it uses the frequency spectrum above 100 GHz, device fabrication goes below micrometer scales.

Traditionally, RF transmission is based on two major technologies

- Waveguide Technology

- Microstrip Technology

Components are manufactured using afore mentioned technologies so far. But these technologies are difficult to implement and device fabrication is not an

economical option. Therefore a need for a transmission technique is felt that can cope up with today's challenges.

Several attempts are made to design new technologies for RF applications e.g. SIW (Substrate Integrated Waveguide), Gap waveguide etc. This report is based on gap waveguide technology. Gap waveguide is a new technology developed for the transmission of radio waves at high frequencies. The heart of this technology lies in designing a PMC surface such that it can allow the propagation in the desired direction, while completely obstructing the propagation in any other direction. A more detailed analysis of this technology will be presented in the following chapters.

1.2 Conventional Waveguides

Metal waveguides as shown in figure 1.1; exist in the field of microwave since early 19's. Waveguides are metallic structures of rectangular or cylindrical shape defined by a specific cutoff frequency. The dimensions of these structures define their range of operation. Waveguides are usually manufactured according to the international standards over different frequency bands.
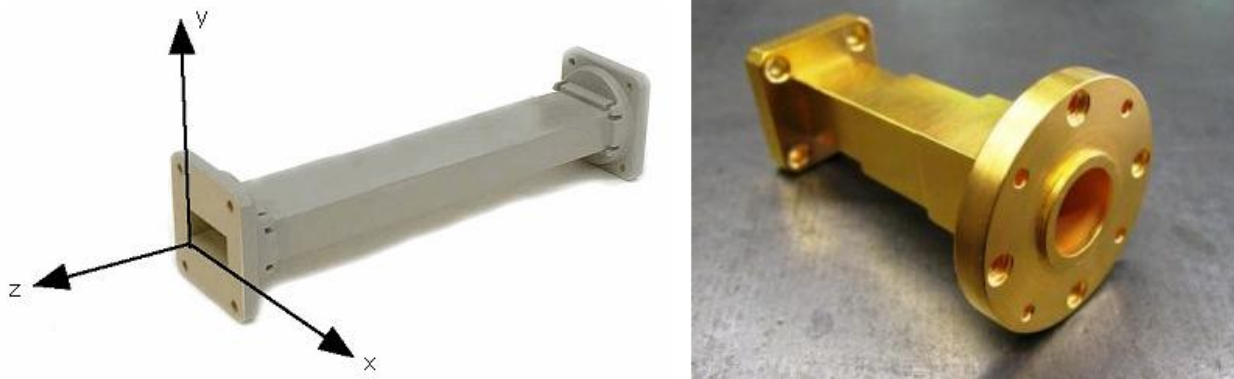
Figure 1-1 Rectangular and Circular Waveguide

Using waveguides, many useful components are designed such as Magic tee, circulators and couplers, as this report concerns couplers only, so we will confine ourselves to this particular component. Couplers are widely used in microwave applications. At frequencies higher than 30 GHz, usually couplers are

manufactured in two parts and later joined using screws. These couplers can work up to 60GHz but to provide electrical contact and water proofing simultaneously is not economical. Moreover, due to mechanical imperfections, electric field leaks through them and thus degrades the performance. These problems are more explained in the coming sections.

1.3 Design Specifications:

The purpose of this master thesis is to design a 3dB coupler using gap waveguide technology around the center frequency of 38.5GHz for a bandwidth of 7%. The proposed electrical specifications of the coupler are as follows:

Frequency Band	37-40 GHz
Coupling Required	3dB
Isolation	-20dB
Input Matching	-20dB
Waveguide Flange	WR28

There were some proposed mechanical design requirements also, which will be discussed in the last section of this thesis. Here we skip mechanical aspect of the design for brevity.

1.4 Advantages expected from this Design:

The existing couplers are based on conventional waveguide technology. It's a hollow waveguide structure, which is broken into lid and ground plate such that there is an electrical contact between these two components. Provision of a good electrical contact between two side by side hollow waveguides is mechanically difficult, due to the presence of thin wall between these two structures. On the

other hand, gap waveguides do not require any electrical contact between the top lid and bottom plate. Therefore, a need was felt to utilize this unique feature of gap waveguide technology.

Another difficulty with conventional technology was the requirement of waterproofing of the structure. Water proofing is usually achieved by providing a silicon layer at the edge of the waveguide. Electrical contact together with water proofing poses some serious structural challenges. While gap waveguides provide enough space for such water proofing requirements. One other advantage of gap waveguides is that different transitions such as bends are easy to provide in gap waveguides and still the structure can be planar.

This project is an attempt to encompass all these advantages and yet providing promising performance.

2 Chapter 2

2.1 Couplers

Coupler is a four port passive device, which is used to couple the power from input port to two out ports, while the fourth port is isolated. Figure 2-1 shows a coupler with four ports, where port 1 is the input port, port 2 and 3 are the output ports while port 4 is the isolated port. This device is completely symmetric, therefore any port can be designated as input port and correspondingly the other port combinations can be determined.
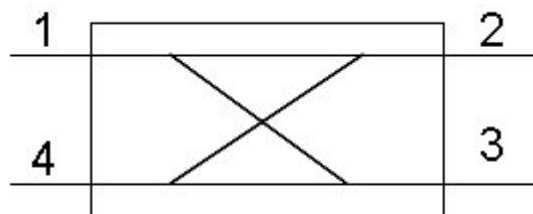
Figure 2-1 Ideal Coupler

These couplers are often called directional couplers due the fact that output ports can only be assigned according to the input port. Power flows in a specific direction, while no power is reflected back at any port. Therefore a directional coupler is ideally matched at all ports. In RF literature, ports are normally named for generalization. These port names are relative to the input port. For example, in Figure one if we select port 1 as input port, then port 2 is through port, port 3 is coupled port and port 4 is isolated port. Ideally all the power is divided between through and coupled port while no power is available at isolated port. From here onwards, ports will be referred by their names instead of numbers.

2.2   Performance Parameters

As performance measures, certain parameters are defined for couplers. These parameters will be used during this report, so a brief definition is provided here. For detailed definitions, reader can consult [19] .

2.2.1   Insertion Loss

Insertion loss is defined as the ratio between the power at input port and through port. Insertion Loss is often expressed in dB.

2.2.2   Coupling Factor

Coupling factor is the amount of power coupled to the coupled port. It is often defined as the ratio of incident power and coupled power. Coupling factor is also expressed in dB.

2.2.3   Isolation

Isolation is defined as the ratio between the power at input and isolated ports. It determines the power travelling in the backward direction. It is also expressed in dB.

2.3 Types of Couplers:

Couplers can be divided mainly into two categories.

- Forward Couplers

- Backward Couplers

If the power is coupled at the coupled port then it is called a forward coupler, similarly if the power is coupled to the isolated port then it is knows as backward couplers. Of course the port names are interchanged in case of a backward coupler. In this report we will focus on forward couplers. Backward couplers are not much of interest for this report.

Couplers are implemented usually in waveguide or microstrip technologies. Striplines are also used for couplers. Examples of microsrtip couplers are branch line couplers, rate race etc. In waveguide technology, bethe-hole and short slot couplers are widely used. This project is more concentrated on waveguide technology, so we will not present microstrip couplers in detail.

2.3.1 Bethe-hole Coupler:

Bethe-hole coupler is constructed by placing two waveguides on top of each other and providing a hole in the broad wall as shown in Figure 2-2. The radius, shape and distance from narrow wall determine the amount of coupling.
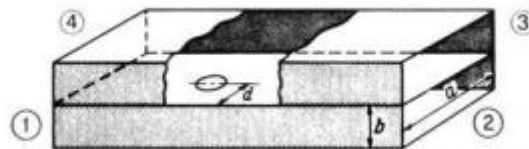
Figure 2-2 Bethe-Hole Coupler

2.3.1.1 Theory of Operation:

Bethe-hole couplers work on the principle of producing a magnetic dipole moment through the aperture, thus inducing a magnetic field in the top waveguide. The theory is explained in section 4.13 of [18]. In a simpler way, coupling can be controlled by varying the radius and distance from the narrow

wall of the wave guide. It is assumed that the hole is located at centre of the waveguide. Following formulas can be used to calculate the radius and location of the hole.

$$C = \frac{20\log(1+X^2)}{X}$$

$$X = (16\pi r_0^3 / 3ab\lambda_g)\sin^2(\pi d/a)$$

In the above equations, 'r' is the radius of the hole, while 'd' is the distance from the narrow wall. Also it is assumed that the guide walls are infinitely thin, meaning that it's having infinite conductivity.

The two wave guide not necessarily should be on top of each other, they can have some angle θ as shown in Figure 3.
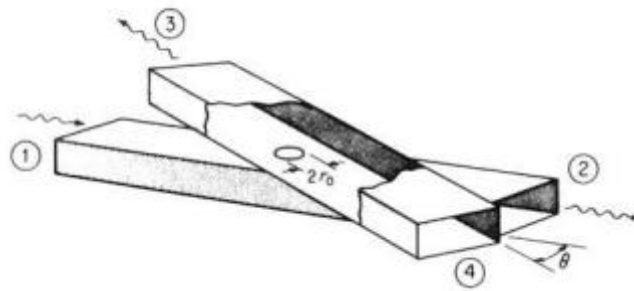
Figure 2-3 Bethe-hole coupler at an angle θ

Moreover, the hole needs not to be circular. The shape of the hole can be rectangular or more commonly cross.

Another way for constructing the coupler is to add multiple holes, thus controlling the amount of coupled power over a certain bandwidth is achieved. The holes are quarter-wavelength apart and this produces zero transmission at port 4.

2.4 Short-Slot Coupler

The Riblet short-slot hybrid coupler is constructed by placing two hollow waveguides side by side and removing a section from the centre wall. The Riblet coupler is depicted in Figure 2-4
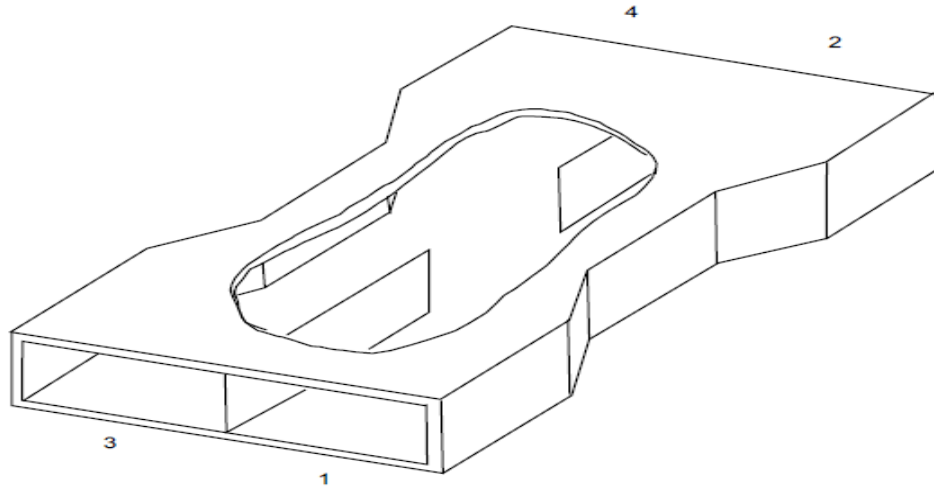
Figure 2-4 Shot Slot Hybrid (Riblet) Coupler

2.4.1 Theory of Operation

In the above figure a portion of the middle wall is removed thus there is a double-width waveguide in which both the TE20 mode and the TE10 can propagate. (The width is sometimes narrowed, as shown, to keep the H30 mode from propagating). This width can be calculated by solving the following equation for a TE20 mode.

$$f_{c,nm} = cn/2a$$

Where 'a' is the broad dimension of waveguide and 'n' is the number of maxima in x-direction. Note that we do not want electrical field to vary in y-direction, that's y there is no maxima in y direction. Length of the coupling section is significant in determining the coupling ratio of the coupler. For a 3dB coupler it is estimated that the coupling length should be greater than the half wavelength at the centre frequency.

$$L_{coupling} > \lambda_g/2$$

By choosing the length of the removed wall section properly, an equal division of the power incident can be obtained with a good match at all ports. The forward-going wave in the coupled guide has in addition a phase shift of 90˚, whereas there is no backward-going wave in the coupled guide. The theory of operation is fully explained by Riblet [14] and [15]. In order to have a good match a capacitive dome is provided in the middle of coupling section. The number of steps of indentations determines the band width of the coupler. A wide band designed is presented in [15]. This design utilizes three indentation sections with decreasing lengths. Riblet couplers usually provide a 90˚ phase shift that is the reason it is known as hybrid coupler.

Another way of constructing the coupler is by providing the holes in the middle wall. This type of arrangement resembles Bethe-hole. Such a design is difficult to realize and cannot provide a good coupling for wider bandwidth [14].

2.5 Branch Line Couplers

Branch line couplers are basically microstrip couplers. In micróstrip, it's easy to define impedance of a line; therefore branch line couplers are constructed using combination of two different impedance lines. A simple branch line coupler is illustrated in figure 2-5.
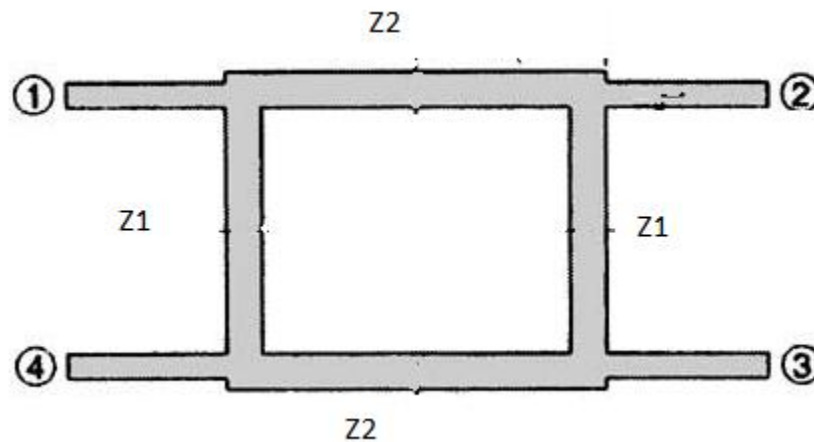
Figure 2-5 Branch Line Coupler

A branch line coupler uses quarter-wavelength lines with two different impedances as shown in the above figure. The ratio between the impedance depends on the amount of coupling required. A more detailed discussion can be found in [18].

3 Chapter 3

3.1 Gap Waveguides

Hollow waveguides have been a medium for transmission of RF. Hollow waveguides are metallic structures of any definite geometrical shape rectangle or cylinder. The dimensions of these waveguides depend on the operation frequency. These relations can be found in [18] and [19]. Hollow waveguides are available from 3-80GHz, but more commonly they are used for 3-30GHz transmission. They have the advantages of low loss and can withstand high powers. On the other hand, when the frequency increases beyond 30GHz, the dimensions become too small and difficult to realize in metal structures. Although the microstrip structure is available for high frequencies, yet it has the additive disadvantage of loss due to substrate. Therefore, a waveguide is more desirable at high frequencies.

Many attempts have been made to overcome this problem of small dimensions in waveguides. An example of which is SIW (substrate integrated waveguide). SIWs are manufactured between two ground planes separated by a dielectric. Side walls are provided using via-holes between two ground planes. This structure is capable of supporting higher frequencies, yet the loss is high due to the substrate involved.

3.2   Soft and Hard surfaces

The electromagnetic properties of a conducting surface can be altered by incorporating a special texture on the surface which helps in describing the surface with a single parameter termed as its surface impedance. Magnetic conductivity does not exist naturally but can be realized in the form of high surface impedance. The first conceptual attempt to realize high surface impedance was the so called soft and hard surfaces [7], where they were defined in terms of their anisotropic surface impedance.
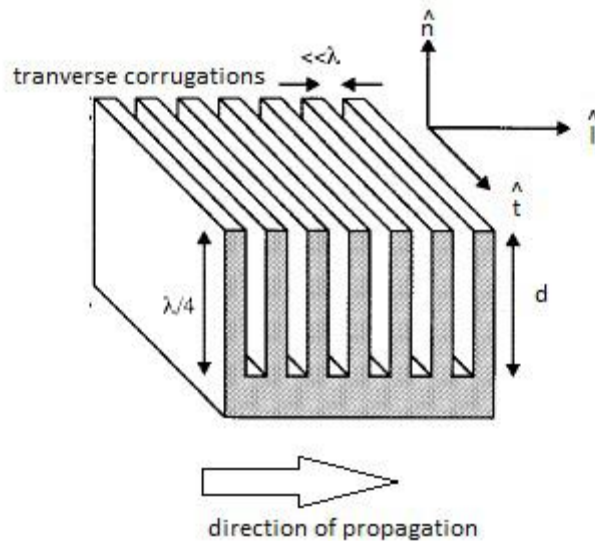
Figure 3-1 Transversely Corrugated Soft Surface

Figure 3-1 describes a transversely corrugated soft surface with two principal directions both being tangential to the surface: the longitudinal direction $\hat{l}$ which

is in the direction of the pointing vector and the transverse direction $\hat{t}$ orthogonal to it. The longitudinal and transverse surface impedances are given by

$$Z_l = -\frac{E_l}{H_t} \qquad and \qquad Z_t = -E_t/H_l$$

From the knowledge of transversely corrugated surfaces we can uniquely define a soft surface by

$$Z_l = 0 \qquad and \qquad Z_t = Infinity$$

A grid of parallel PEC / PMC strips, where every second strip is PEC and PMC respectively [3] is used now a day to describe the ideal soft and hard surfaces. They are characterized by their anisotropic boundary conditions that allow an arbitrary polarized wave to propagate along the strips (hard surface case) whereas they stop wave propagation in directions orthogonal to the strips (soft surface case). High impedance surfaces with a forbidden frequency band have been discussed in detail in [8]. Due to the isotropic boundary conditions, the EBG surface [8] stops wave propagation in all directions. Fakir's bed of nails refers to a two dimensional array of metal pins [2] arranged on the conducting surface, which mimic the ideal impedance surface boundary. It has been demonstrated in [9], that by placing the structure in between two parallel plates and varying different parameters typically the gap height, can produce extremely large band gap (parallel plate stop band)(2.5:1) to prevent wave propagation. The surface impedance is very high in the band gap, so the tangential magnetic field is small, even with a large electric field along the surface. Such a structure is sometimes described as a magnetic conductor.

3.3 PMC Realization using bed of nails

In fact there are many ways of realizing parallel plate stop band, which have been compared in [10], but gap waveguides introduced in [1] and experimentally verified by use of bed of nails [2], as a high impedance surface for parallel plate

mode suppression. Fig. 3-2 has been taken from [11] in order to motivate the need for using bed of nails as a high impedance surface in gap waveguide technology. The 2-D color plots show the suppression of different cavity modes as well as the strong fields in the bends of the microstrip line within the stop band(Octave bandwidth) when the lid of nails is employed. It can be observed that the mode suppression has a bandwidth of more than 2:1 and it does not interfere much with the microstrip circuit. Therefore this mode suppression technique has introduced a new advantageous packaging technology for high frequency circuits.
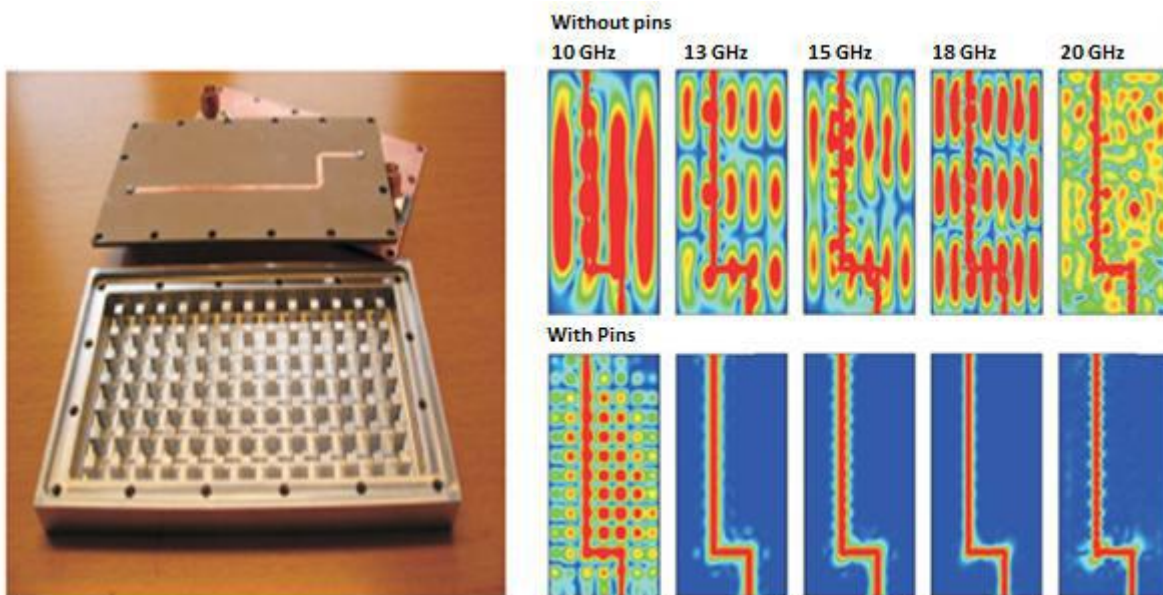
Figure 3-2 Manufactured metal lid with pins (left), 2-D color plots of vert. E field Distribution (right) inside the gap between the microstrip board and the lid of the metal Box, both (a) with smooth metal lid and (b) with a lid of nails [11]

The metal pins can be easily milled in the same way as the conducting ridge can be. Such manufacturing allows varying the height of the texture, thereby providing more degrees of freedom in a design process than substrate bound alternatives. Furthermore it is believed that it is possible to integrate active and passive components like amplifiers and MMIC's even in the form of unpackaged semiconductors chips, which should be easy because the metal pins may also work as heat sink, provide cooling, shielding and packaging at the same time. A

comparative study for investigating the PMC realizations[10], has motivated the need to use bed of nails approach, providing band stop for more than an octave band, furthermore this technology is having less loss, cheap and easy to mill.

3.4   Waveguide Implementation using High Impedance surface

In the above explained bed of nails, we can alter the structure in such a way that only a desired frequency can propagate and rest of the frequencies is stopped. Two types of approaches are implemented:

- Ridge Gap waveguide

- Groove Gap waveguide

Both of these techniques are explained in the sections below.

3.4.1 Ridge Gap waveguide

The propagation characteristics along soft and hard surfaces are very well known, either when they are introduced in hollow waveguides or as open hard and soft surfaces. [3]. The detection of local surface waves along each groove of a hard surface, introduced in[12], has been followed by the detection of local modes along the ridges of a longitudinal corrugated hard surface, when a smooth metal plate, separated by a narrow gap was located over it[13]. This has resulted in a new way of killing higher order modes [13], by introducing the hard surface in a TEM parallel-plate waveguide. The geometry in [13] has been simplified and improved in [1] to introduce a new basic waveguide confined in the gap between parallel plates.

3.4.1.1 Principle of Operation

The principle of operation of the gap waveguide is based on the following theoretical facts that are either well known or can readily be derived from Maxwell's equations

- If the gap height 'h' between a PEC and a PMC surface is less than a quarter wavelength, the wave propagation becomes prohibited in any arbitrary direction.

- Wave propagation in any direction can be made prohibited, in between a PEC and an EBG surface if the gap height is typically small. This gap height depends upon the geometry of the EBG surface and it is found to be less than a quarter wavelength as well. The PEC boundary conditions between the parallel plates for horizontal polarization provides cut-off whenever h < λ/2, which is a weaker cut-off condition than h < λ/4, which is valid for the PMC boundary condition on the lower plate.

- Waves in the gap between a PEC surface and a PEC/PMC strip grid can only propagate along the direction of the PEC strips whereas they are in cut-off for vertical(TM) and horizontal (TE) polarization when h < λ/4 and h < λ/2 respectively. Therefore an ideal gap waveguide works for all frequencies up to a maximum defined by h = λ/4.

The bandwidth of the propagating wave along the ridge can be estimated from the frequency band over which the propagation constant in directions away from the ridge is imaginary, corresponding to an evanescent wave. For the special bed of nails EBG surface used in [1], the PMC appears ideal for thin pins and small periods when the pin length d = λ/4 and the band gap is at high frequency limited by a TE wave starting to propagate when d+h = λ/2. From the comparative studies of [10], it was possible to design gap waveguides with octave bandwidth (2:1). Figure 3-3 has been taken from [1] showing the dispersion diagrams for the gap waveguide to justify the above discussion related to its band stop characteristics. The dispersion diagrams in Figure 3-3(a) and Figure 3-3(b) were computed without ridges for infinite periodic structure and finite dimensions in transverse plane with PEC side walls respectively, showing a large stop band above 10 GHz where no waves can propagate. The basic parallel plate mode that started at zero frequency as a TEM mode is represented by the left curve in Figure 3-3 (a). This mode is then deviated from the light line and went into cut-off just below 10 GHz. It appeared again at 23 GHz together with another mode. Several rectangular waveguide modes appeared below 10GHz, when metal walls were introduced, limiting the transverse extent of the parallel plate geometry in Figure 3-3 (b). These modes have a lower cut-off similar to normal rectangular waveguide modes

but went into a stop band just below 10 GHz and appeared again at the end of this parallel plate stop band at 21 GHz. The dispersion diagram of Figure 3-3(c) includes the ridge as well. The diagram which relates the introduction of the ridge shows a new mode propagating closely to the light line, in fact following the ridge within the whole parallel plate stop band. This is the desired quasi-TEM mode and it is termed as quasi-TEM because it follows the light line very closely but not exactly. Another higher order gap waveguide mode appeared at 19 GHz, having a vertical E field distribution with asymmetrical sinusoidal dependence across the ridge, being zero in the middle of the ridge.

(a) Infinite pin structure
(b) Finite pin structure with PEC side walls
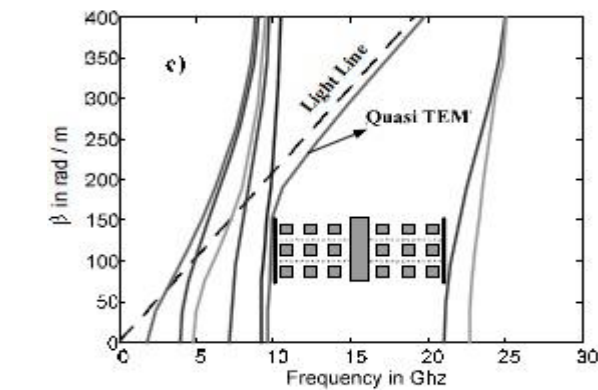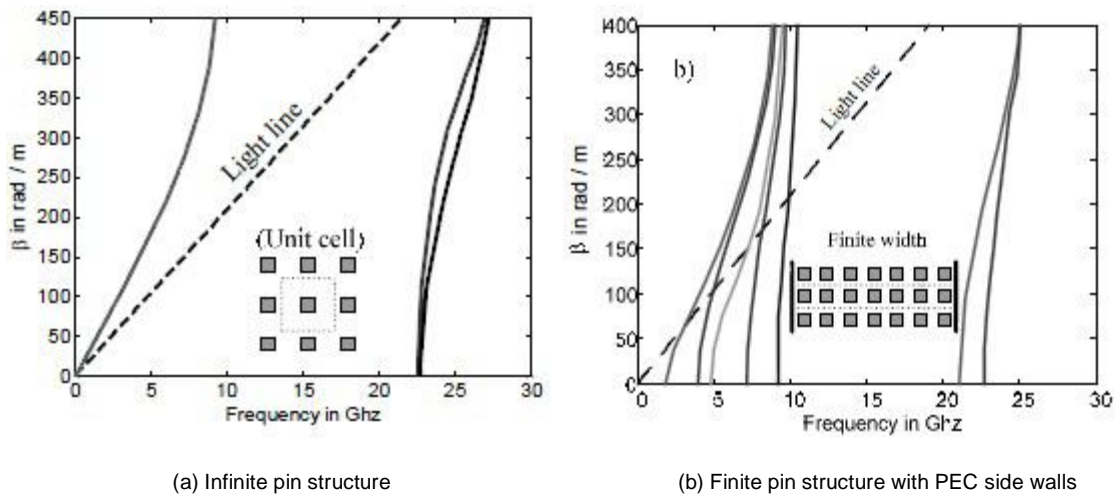
Figure 3-3 Dispersion diagram for the gap waveguide [1]

3.4.2 Groove Gap Waveguide

The groove gap waveguide is designed on the same principle as explained in the above sections. Its uses the same high impedance surface (bed of nails) to

implement EBG concept. The difference between ridge and groove gap wave guide is that in groove gap waveguide field propagates in the interior of a groove created in the textured surface instead of along the top of a ridge [13]. The boundary conditions for the field in the groove are the ones given by four metal walls, but with the equivalent of a magnetic conducting strip in each of the corners between the upper horizontal plate and the two vertical metal walls. Consequently, the groove is expected to allow the propagation of modes in a similar way as in hollow rectangular waveguides, i.e., with a cutoff frequency given by the groove dimensions. Due to these similarities, this groove can also potentially be used to design horn antennas radiating from apertures between the two contactless parallel plates. It would be advantageous if such horns could radiate two polarizations (perpendicular and parallel to the plates, referred to as vertical and horizontal polarizations, respectively),

(a) Vertical Polarization

(b) Horizontal Polarization
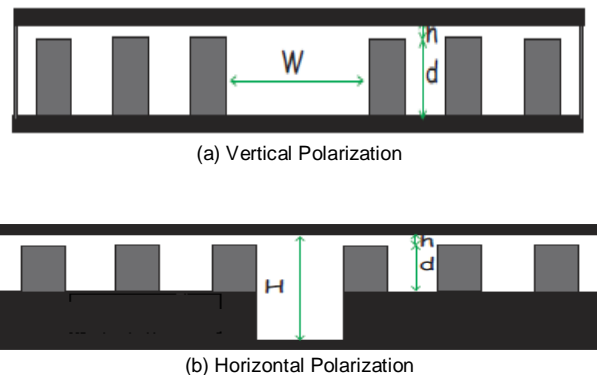
Figure 3-4 Cross-sections of the groove gap waveguide for vertical and horizontal Polarizations for vertical and horizontal polarizations. The grey areas are metal Pins (periodic along z-axis), and the black areas solid metal[14]

3.4.2.1 Principle of Operation

Groove gap waveguide is an alternate of rectangular hollow waveguide. It can support TE and TM modes. The dimension of the groove determines the cutoff frequency, guided wavelength and propagation constant. We can easily apply all the formulas of rectangular hollow waveguides to groove gap waveguides.
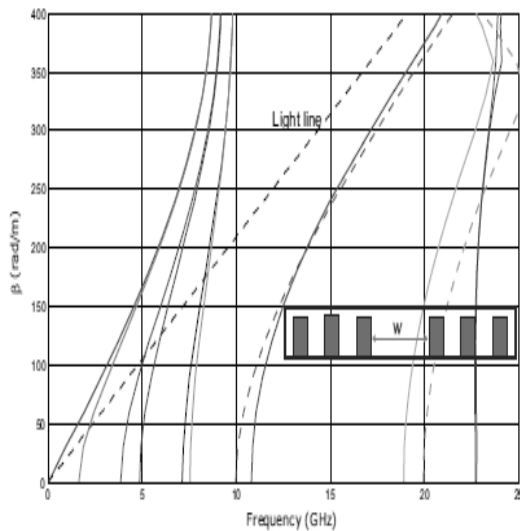
(a) Horizontal groove   (b) Vertical groove
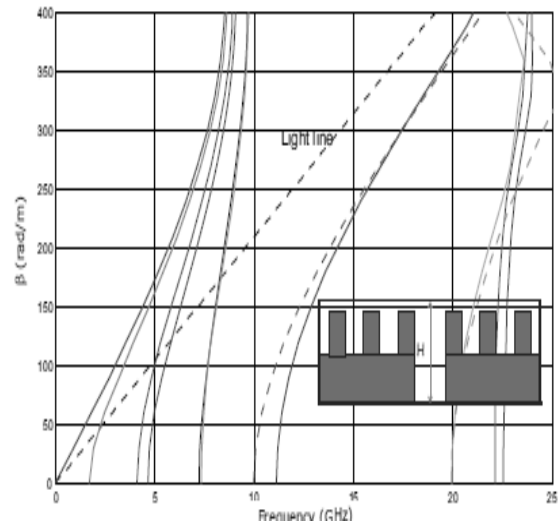
Figure 3-5 Dispersion diagrams for three different structure Dashed lines in subfigures a and b are the modes of an ordinary rectangular waveguide with same dimensions as the groove[13]

If we now compute the field distribution in the cross section of the two types of groove waveguides for a frequency within the desired "monomode" band (15GHz) we achieve the results shown in Figure 3-6. For the vertically polarized case we observe a field distribution similar to the one of a TE10 mode in an ordinary waveguide, with the electric field vertically polarized with respect to the plates. When the groove is vertically oriented, the field distribution is a cosine type with mainly horizontal polarization (parallel to the plates) as expected. Another important aspect derived from these 2D plots is the fact that the field is quite confined on the groove. From the plots we can see that after the second row of pins the field is negligible. Thereby if some of these waveguides are manufactured sharing the same plates, they can be highly isolated requiring only few rows of pins between them to this aim. This allows the design of arrays of waveguides with low coupling between neighboring ones without requiring any metal contact between the two plates.

(a)   Horizontal waveguide

(b)   Vertical waveguide
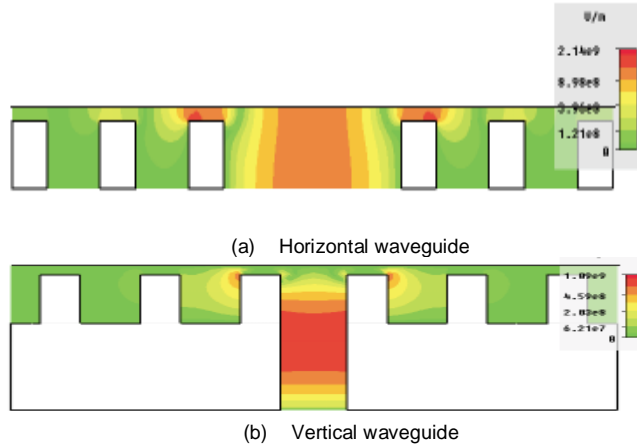
Figure 3-6 2D color plots of the transverse Electric field for frequency within the single mode band (15GHz)[13]

As the groove gap waveguide is identical to rectangular waveguides. It was chosen to implement the desired coupler, which will be explained in the coming chapters.

4 Chapter 4

4.1 *Coupler Design and Simulation*

So far we have explained the technology and concept required to design the coupler. In this chapter we will layout the actual design procedure and the theoretical basis to proceed in future. All the simulations were performed in HFSS v12.0. The initial design was implemented without taking into account the size and measurements consideration. The final design of the coupler will be explained in chapter 5.

4.2 Groove Gap waveguide Implementation

The first step is to implement the concepts explained in chapter 3 in HFSS. As we know that gap waveguides can be implemented in two ways as explained earlier. Therefore it was possible to proceed with any technology (i-e ridge or groove). We have chosen groove gap waveguide due to the fact that Arkivator is having the current design implemented in rectangular hollow waveguides. As groove wave guides are identical to rectangular waveguides, it will be easy to compare the results for both of the designs. Moreover, in groove gap waveguide, we need not to design transitions (i-e from rectangular waveguide to Ridge waveguide and vice versa). Therefore Groove waveguide was chosen due its simplicity and ease of manufacturing.

The groove waveguide was implemented first by using the dimension given in [reference]. Following are the dimensions used for initial Groove waveguidedesign.

Pin Size(mm)	Groove Width(mm)	Air Gap(mm)	Pin Period(mm)	WG Length (mm)	Material
3×3×5	15.8	1	4	45	Copper

Table 1
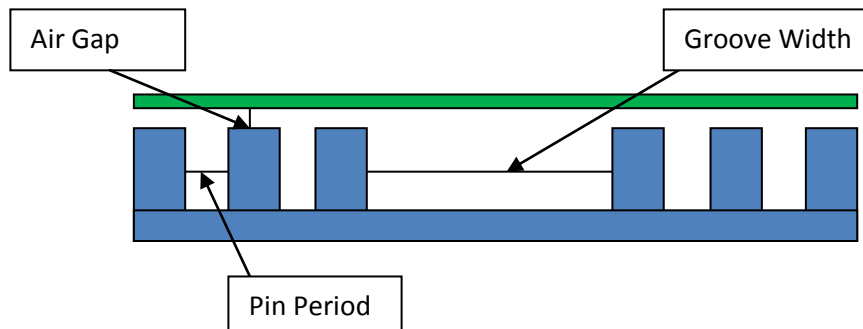
Figure 4-1 Cross-section of Groove waveguuide

Although it is established in chapter 3, that 2 rows of pins on both side of groove is enough but we have used 3 rows, in order to provide good isolation in case of an adjacent waveguide. The simulated results for this structure are presented in Figure 4-2.
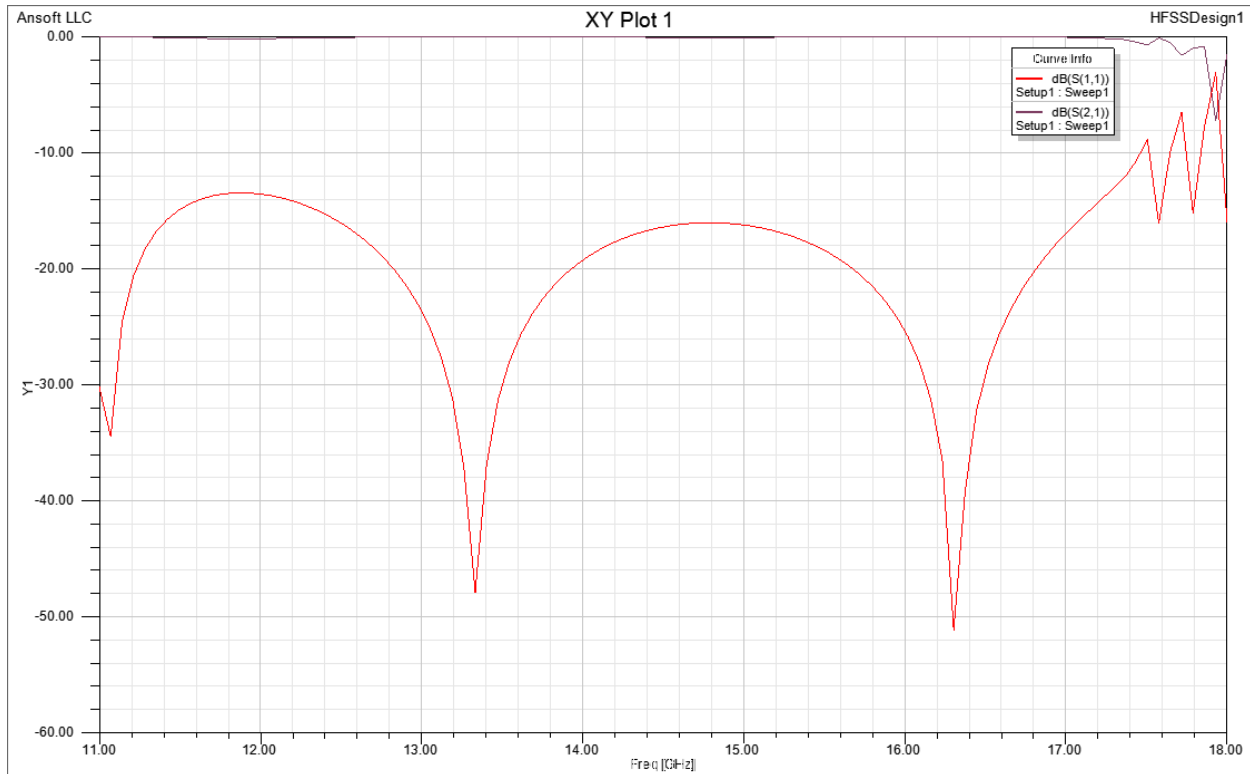
Figure 4-2 S11 and S21 for Single Groove Gap waveguide

From the simulation results, we can see that Groove waveguide is working from 11-17.5GHz with a good return loss (S11). Although at the edge of the band we can see resonances. But the performance can be improved by tuning the dimensions of this waveguide.

Now we have to place the two waveguides adjacent to each other, so that we can have coupling between them. But as a starting point, we want to have good isolation between these two waveguides. Figure 4-3 shows the cross section of 2 Groove waveguides lying adjacent to each other.
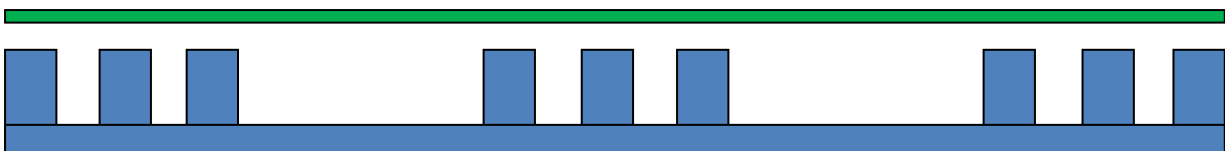
Figure 4-3 S-Cross-sectional View of two Groove Gap waveguides lying side by side

Both waveguides are isolated using three rows of the pins. The dimensions used here are the same as table 1. For this structure we had the following result.
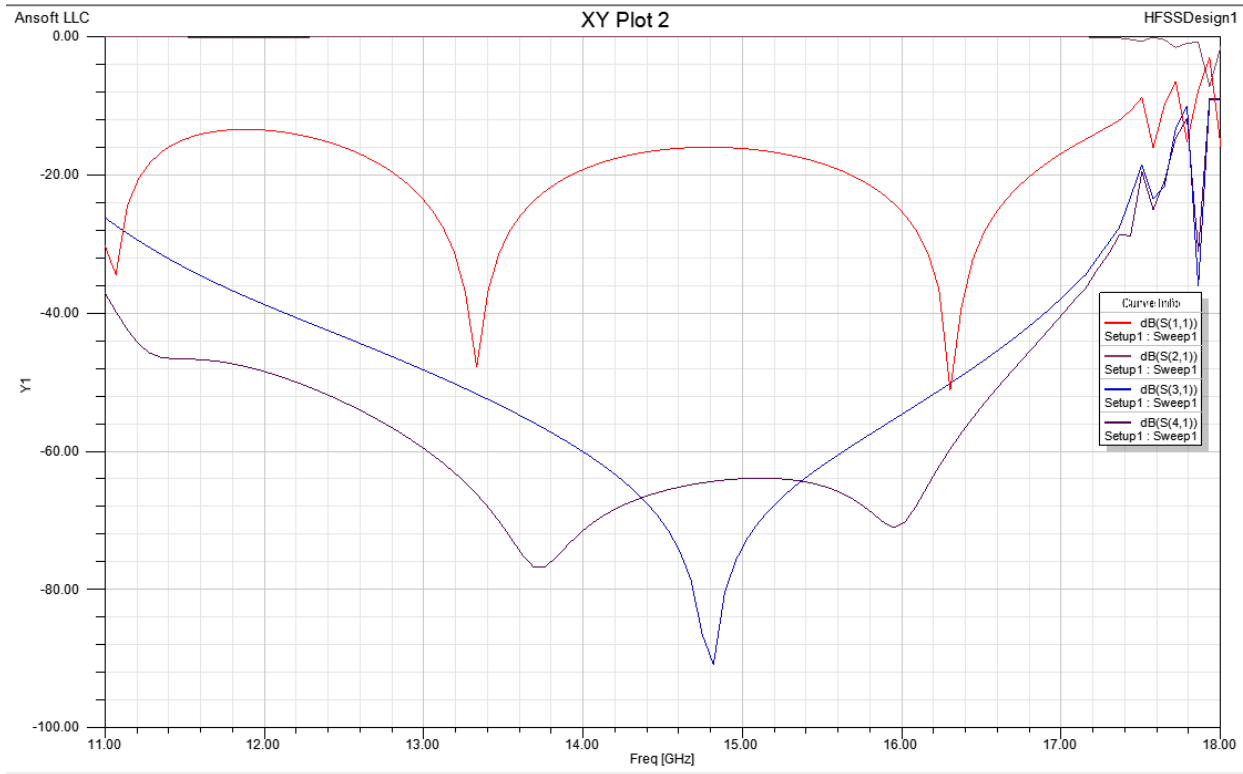
Figure 4-4 S-Parameters for two Groove Gap waveguides lying side by side

From Figure 4-4, it is evident that isolation between two waveguides is less than -30dB over the entire band. Therefore, it is possible to place two waveguides side by side and yet can have a good isolation.

The above mentioned simulation was meant only for 11-18GHz. In order to move to our desired frequency band, we need to scale down the dimensions so that waveguide can work in the band of 37-40 GHz. Following are the dimensions chosen for our groove waveguide.

Pin Size(mm)	Groove Width(mm)	Air Gap(mm)	Pin Period(mm)	WAVEGUIDE Length (mm)	Material
0.62×0.62×2.06	6.539	0.413	1.03	45	Copper

Table 2

Table 2 gives the values which will provide the best results in our desired band. We can observe that all the values are not exact multiples of the values of table 1. The reason is that we have tuned the dimensions in such a way that we can have

minimum reflection and isolation at our desired band. Figure 4-5 shows the results for above dimensions.
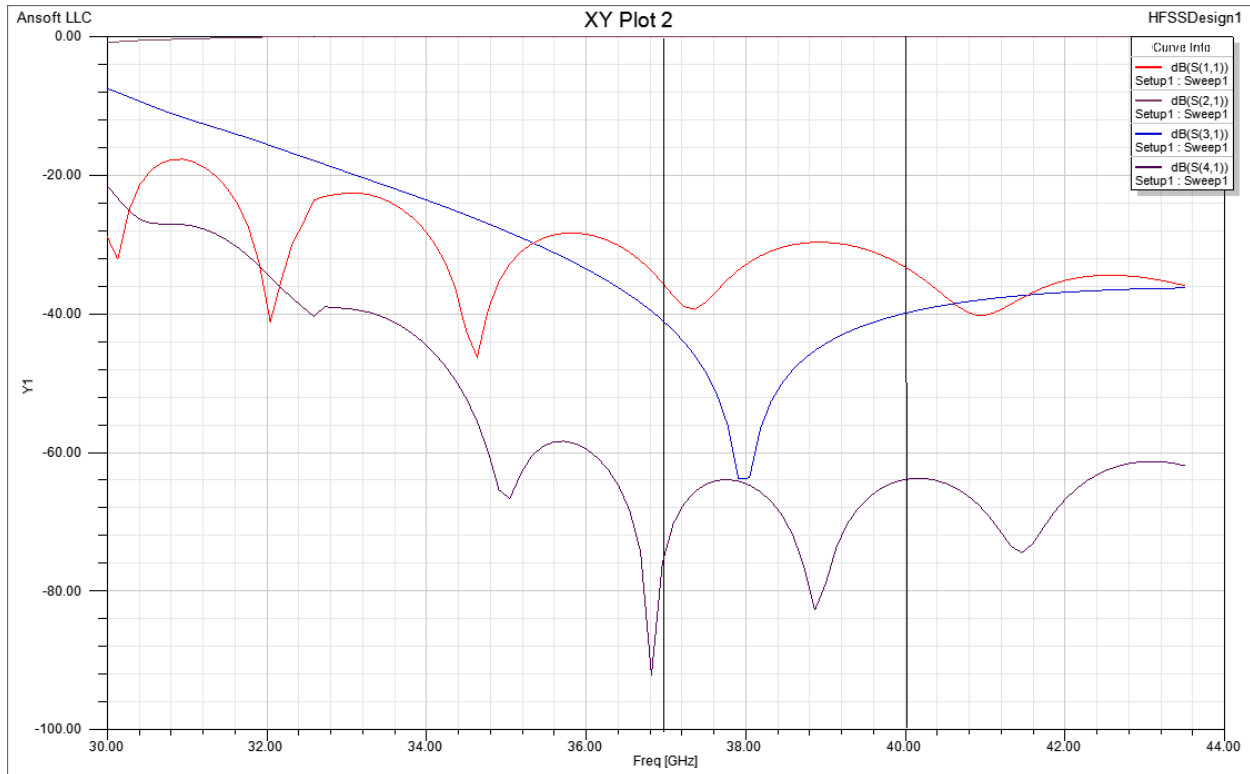
Figure 4-5 Optimized S-Parameters for two Groove Gap waveguides lying side by side

Our groove waveguide is working from almost 33-43GHz, thus providing the octave bandwidth. In the band of 37-40GHz (between two black lines), reflection is less than -30dB while isolation is as better as -40dB. Therefore, these dimensions are best for our design purposes. Of course, other combinations can be used to shift the frequency band, but we need to keep in mind the manufacturing constraints also.

4.3 Coupler Design

As different types of couplers have been discussed in chapter 2, we can see that a bethe-hole coupler is not possible for the current geometry. As the two waveguides are lying side by side, a short-slot hybrid will be easy to implement. From the earlier discussion we know that in the rectangular hollow waveguides, a section of length L is taken away from the common wall to have coupling. The

thickness of this wall is assumed to be zero for ideal case. In the case of gap waveguide, common wall is the middle three rows Figure 4-3, and we cannot assume it to be zero thickness. Another alternative can be removing one row of the pins, as two rows can provide good isolation. Moreover, the two rows of the dimensions of table 2, constitutes a quarter wavelength distance, which can reduce the effect of reflection of the coupling section.
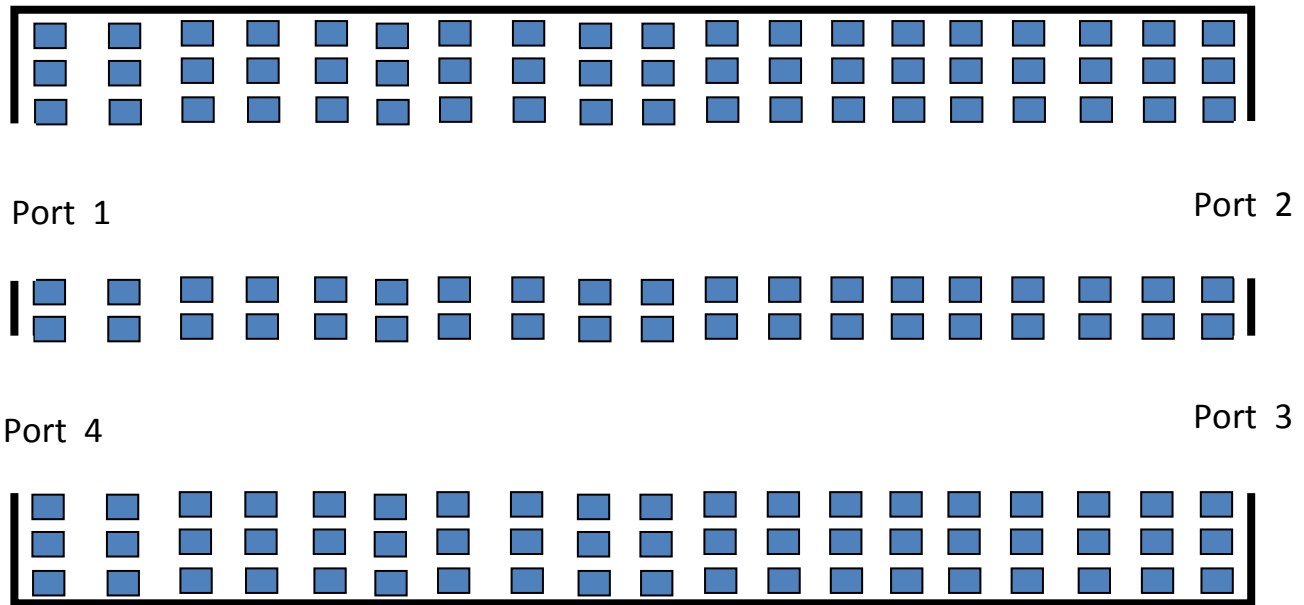
Figure 4-6 Layout of Groove Gap waveguide with port Description

When the structure of Figure 4-6 was simulated, results were identical to Figure 4-5. Moreover, the port names are mentioned in Figure 4-6, which remains same throughout this report.

From the discussion of chapter 2, we know that coupling length plays an important role in defining the total coupling. In order to have a 3dB coupling between port 2 & 3, we need to have a coupling length $\geq \lambda/2$. The guided wavelength on the center frequency is 9.7mm; therefore we used a coupling length of approximately 5mm to start with. To provide the desired coupling length, we can take away three pins from the middle rows, and can adjust the gap by moving adjacent pins inward. When this structure was simulated, we found out that there is 3dB coupling between port 2 and 3, but as the waveguide's

broad dimension is doubled at the coupling section, it causes a big mismatch at port 1. Moreover, the 3dB coupling is not in our desired frequency range. This frequency shift can be adjusted by the length of the coupling section. In order to compensate the width, we know from chapter 2, that indentations are provided in rectangular waveguides, to match the phase of higher order odd modes (TE20). A similar indentation is provided for our structure and also the coupling length is tuned in Figure 4-7. The indentations were provided by adding extra pins to the side walls of coupling section as shown in figure 4-7. For a start, a single row of pins slightly greater than the coupling length was introduced (L1 in Figure 4-7). Then this row was displaced towards the coupling section, keeping in mind that it should not reach the centre of the guide, as a pin in the center of the guide can block the propagation. When the distance of this extra row from the side wall exceeded the normal period of pins, an intermediate section was provided. This intermediate section is denoted as L1 in Figure 4-7. Such indentation sections can be added further to improve the bandwidth. But the distance between the pins gets too small and difficult to realize. The displacement from the sidewall is found analytically. Another alternative instead of indentations can be a pin in the centre of the coupling section with reduced height. This type of structure is not wideband but surely can reduce the manufacturing problems.
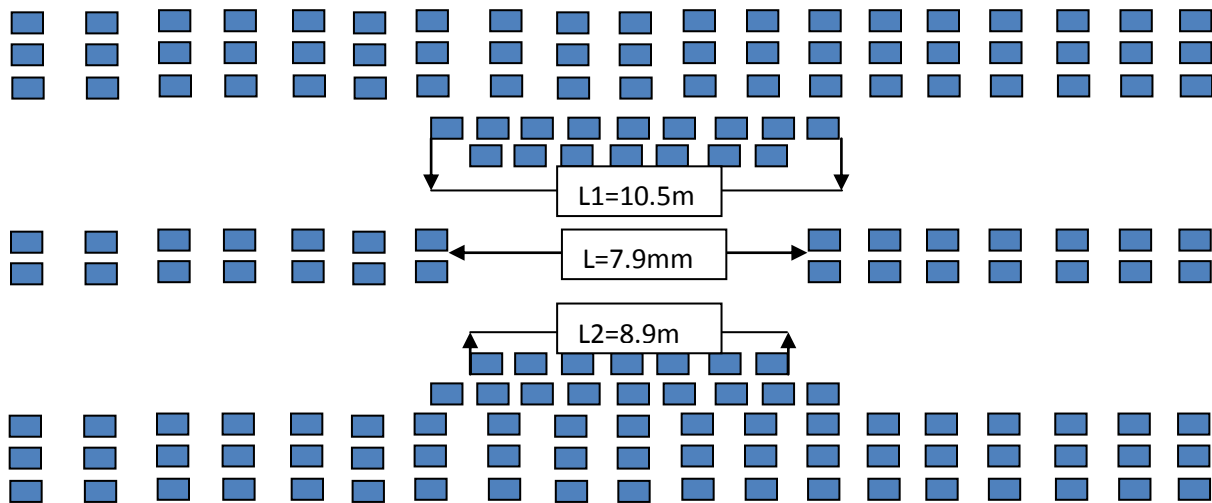
Figure 4-7 Shot-Slot coupler in Groove Gap waveguide

Another alternative instead of indentations can be a pin in the centre of the coupling section with reduced height. This type of structure is not wideband but surely can reduce the manufacturing problems.
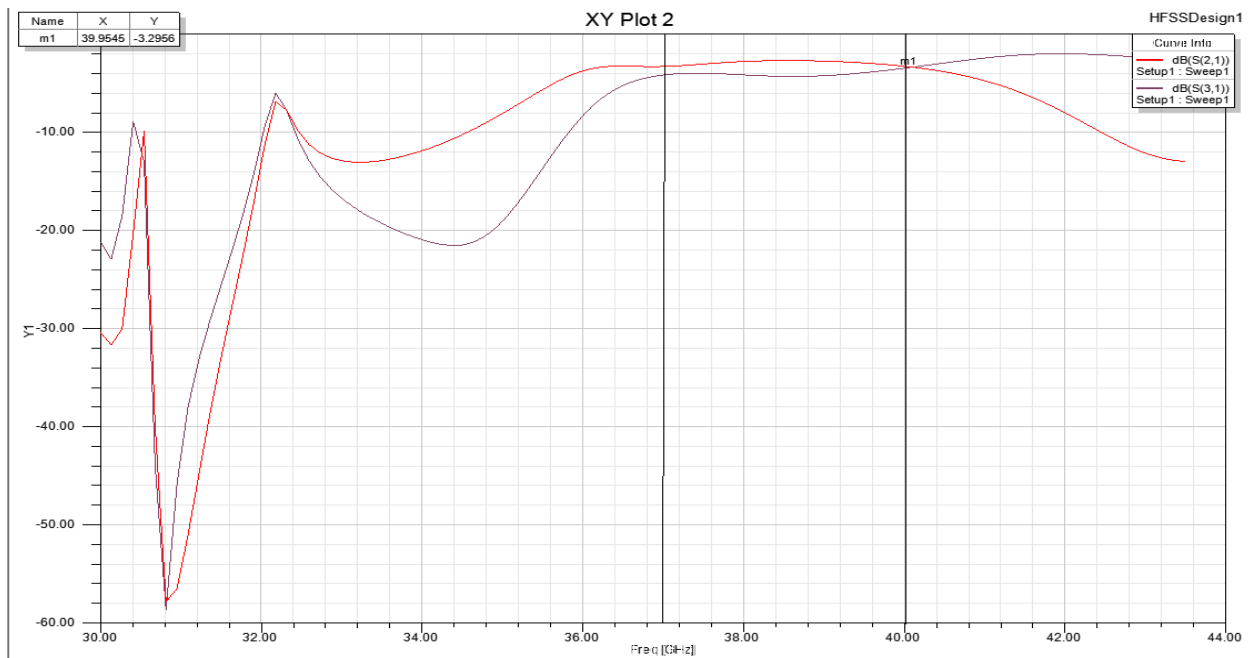
Figure 4-8 S-Parameters for Shot-Slot coupler in Groove Gap waveguide

From Figure 4-8, we can see that the coupling is exactly 3dB at 40GHz. We need to shift this to the centre frequency. Also we need to decrease the amplitude difference of S21 and S31. Moreover, for this configuration, reflection coefficient

and return loss is -15dB. In order to improve all these factors, various techniques can be applied. For example, we can have two extra pins, at the start and end of the coupling sections for a good match, but it was noticed that it increases the amplitude difference. Length of the indentations is also important and the width of the waveguide in the coupling section determines the amplitude difference. To control all these factors we have introduced pucks in the waveguide, which is explained in the following section.

4.4 Matching

Introducing the puck in a rectangular WG means that floor of the WG is made uneven on the selected place. These pucks can be viewed as matching stubs in microstrip structures. The similar can be provided for groove WG. We have introduced pins with reduced height and increased size before and after the indentations. These pins act as a phase balancer for odd mode and also provide a good match at all ports. Positions for these pins were determined by parametric sweep along the length of the waveguide. It was noticed that the height of these pins should be ≤ half of the height of the normal pin, because if we introduce a pin of the same height in the waveguide, it ceases the transmission. Simulation was tried with different number of pins. The best results were obtained by introducing twelve such pins at the four ports. Also the coupling length was optimized for our frequency band. To reduce the amplitude difference, a reduced size pins were provided in the middle of indentation, thus it makes the phase of even and odd mode equal and provides a good coupling. The final structure is given in Figure 4-9
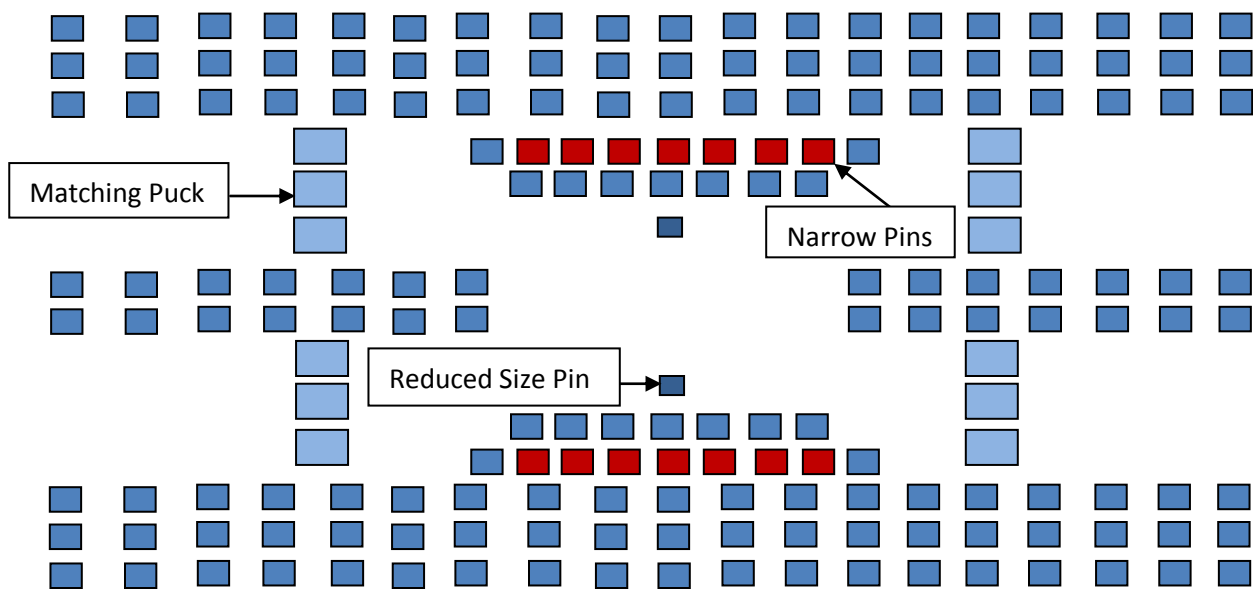
Figure 4-9 Groove Gap waveguide coupler with Matching Pucks

In the above Figure, pins labeled as narrow pins are the pins which can be removed in order to provide manufacturing ease. The dimensions of matching puck and reduced size pins are following:

Matching Puck = 1.02×1.02×0.48 mm

Reduced Pin Size = 0.32×0.32×2.06 mm
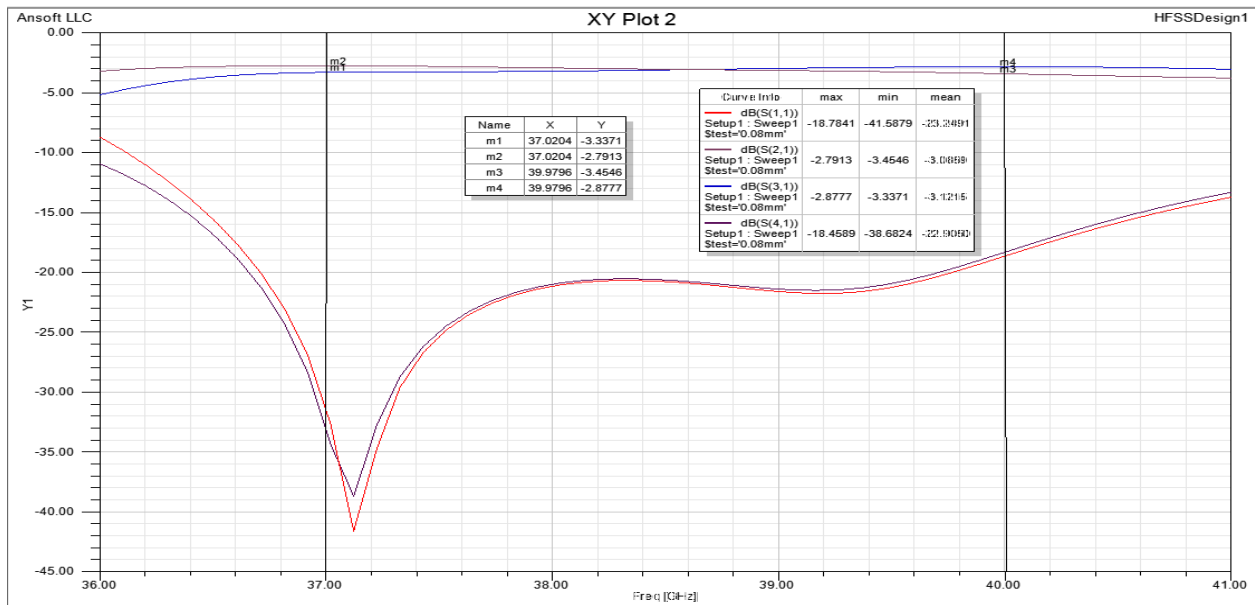
Figure 4-10 S-Parameters for Groove waveguide coupler with Matching Pucks

Figure 4.11 shows the final results for the coupler design. We can see that the reflection and isolation is ≤-20dB over the entire band. The amplitude maximum difference is 0.5dB. Although the phase difference was not included in the specifications, yet we can plot the phase difference of S21 and S31.

It was also observed that the phase difference is 90° over the entire band. So we can safely say that the above designed coupler is a 90° hybrid coupler with a bandwidth ≥7.5%-

5 Chapter 5

5.1 *Mechanical Considerations*

In this chapter, mechanical aspects of the design are considered. As the gap waveguide is a new technology, and measurement techniques are not developed for these waveguides. To be able to measure using conventional methods, we need to have standard rectangular waveguide ports. For mounting these ports, bends are also required. Finally the limitation of milling is also considered. In short we need to transform our design, in such a way that it can interface with existing Microwave Techniques.

5.2 Mechanical Problems

The design presented in chapter 4 is having few mechanical issues. These can be divided into two categories.

- Interface Problems

- Milling Problems

In order to measure the performance of our coupler, we need to address both of these issues separately.

5.3 Interface Problems

Gap waveguide is a newly developed technology. In order to be used with conventional microwave equipment, we need to interface Gap waveguide with rectangular standard ports. All the rectangular waveguides are manufactured according to international standards. This implies that their dimensions must be of a standard size. When we were designing the coupler, we have not taken in to account the dimensions; rather we have just scaled down the dimensions to get the desired result. If we recall the dimensions of our waveguide from chapter 4, we can easily see that we are shorter than the WR28 dimensions, which is a standard waveguide for this frequency band. Our current dimension is 6.539×2.468mm while the standard waveguide is having the dimension of 7.11×3.56mm.

Another important thing is that the distance between the two waveguides is too small. Therefore, a waveguide flange cannot be mounted using this small distance. We need to turn all the ports by 90°, in order to mount a standard flange. Design for bends is discussed in the following sections.

5.3.1 Waveguide Bends

Waveguide bends are characterized as E plane and H plane bends. E plane bends are used when we want to move from a horizontal waveguide to a vertical waveguide such as bethe-hole. In H plane design, bend is introduced in the same plane for both waveguides. As our waveguides are side by side, therefore we need an H plane bend.

H plane bends can be implemented in different ways as discussed in [16]. We have used the cross bend technique to implement $90°$ bend as shown in Figure 5.1
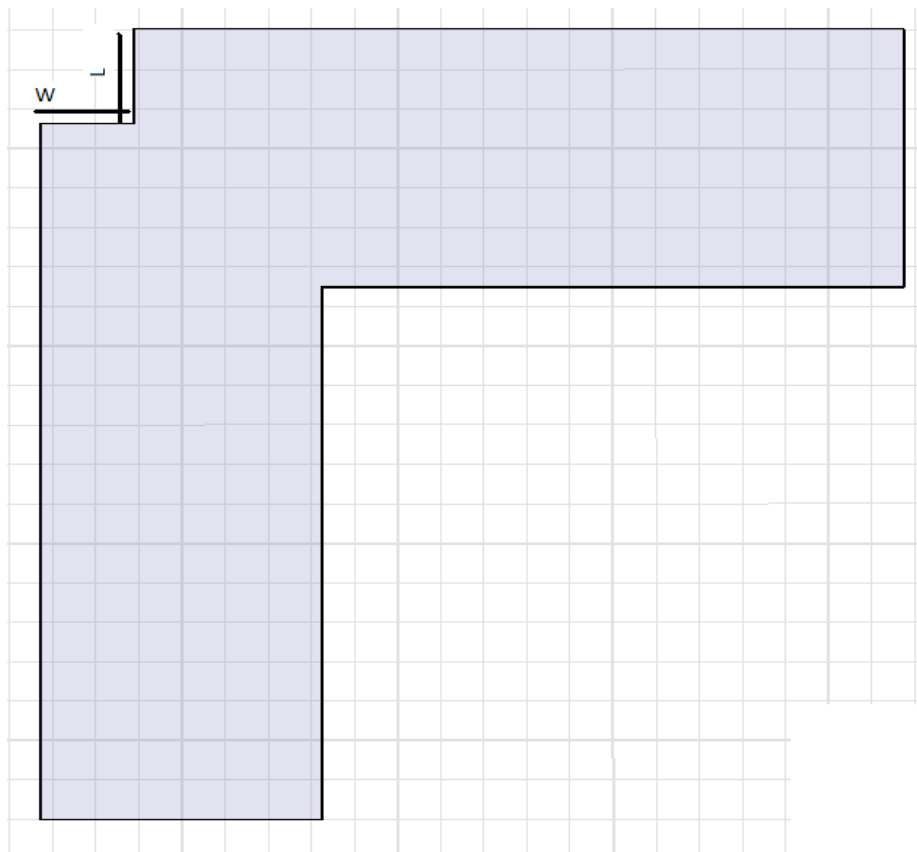
Figure 5-1 Cross H Plane bend for Rectangular waveguide

In the above Figure, two rectangular waveguides are connected using an H plane cross bend. The dimension of the cross W and L determines the bandwidth of the waveguide. The dimensions of waveguides were kept similar to Gap waveguide. Simulated results are plotted in Figure 5.2
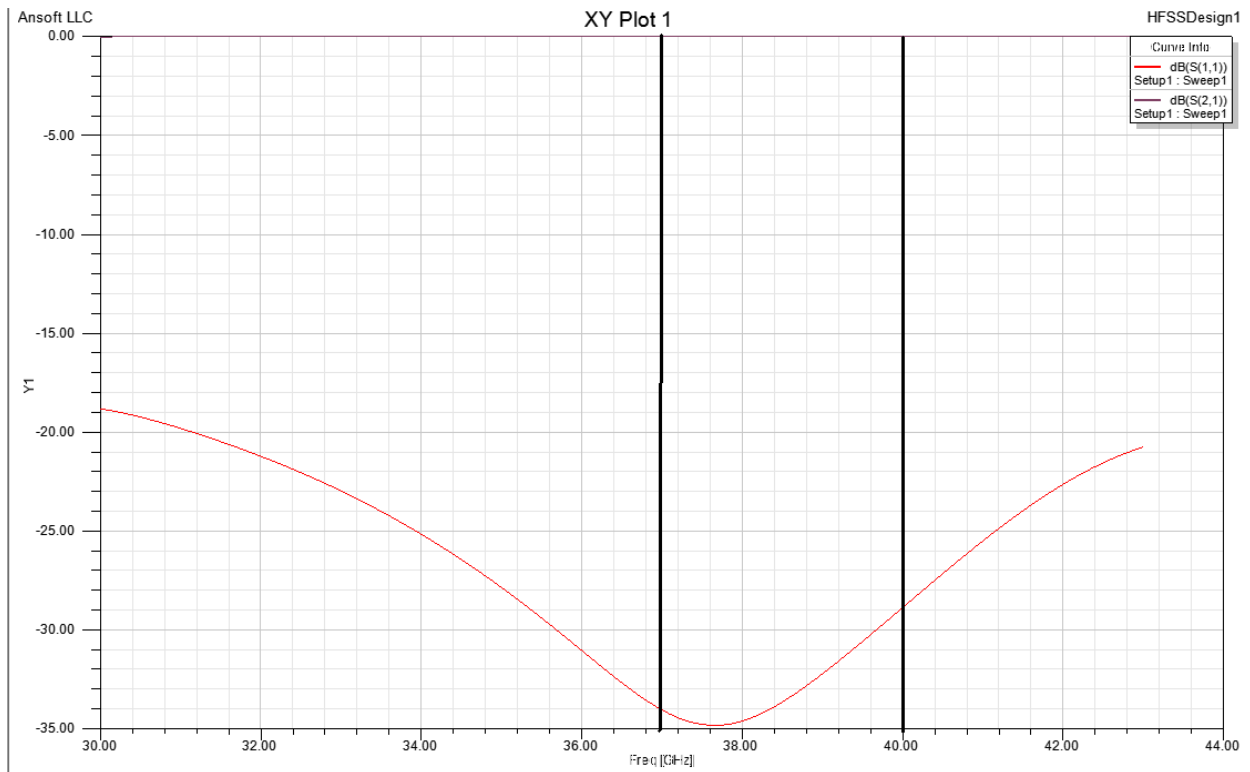
Figure 5-2 S11 and S21 for Cross Rectangular waveguide bend

From the results, we can see that waveguide bend is working from 32-43GHz and with good performance in our desired band. The advantage of cross bend is that the cross can easily be implemented by one pin and therefore can have a simplified structure. Another important feature of the waveguide bend is that it tries to equalize the added width in such a ways that only one higher order mode can propagate though the bend. This property can be utilized to connect two waveguides of different dimensions (difference is only in broad dimension).

We have placed the above bend in our gap waveguide and at the position of cross; we placed the pin with increased size. It was noticed that by moving the position of this pin, we can interconnect two waveguides of different dimensions. Therefore, by parametric sweep an optimized position is selected and has incorporated 4 bends in the normal gap waveguide design shown in Figure 5-3
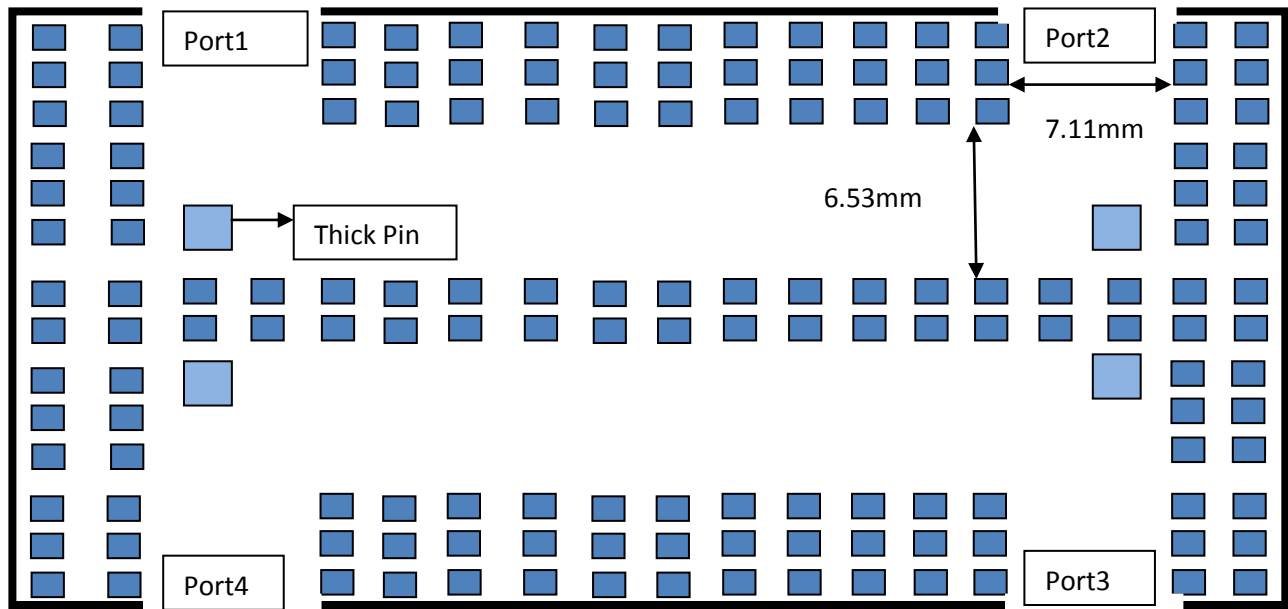
Figure 5-3 H plane Cross bend in Groove Gap waveguide

For the structure of above Figure we can have a reflection coefficient ≤ -30dB over the entire frequency range (37-40 GHz). Moreover, at the output we have the standard broad dimension of the waveguide (i-e 7.11mm).

We will still have interface problem with the narrow dimension of the waveguide. To overcome this, some metal was removed from the ground plate of the gap waveguide. The length of this section was chosen to be quarter wavelength at the centre frequency. To avoid milling effects, two such sections were provided. Layout of the waveguide port is given in Figure 5-4. Finally the structure is simulated by incorporating four such port and result is shown in Figure 5-5. We can see that return loss is ≤ -33dB over the entire range.

Figure 5-4 Groove gap waveguide with Height adjustments Steps
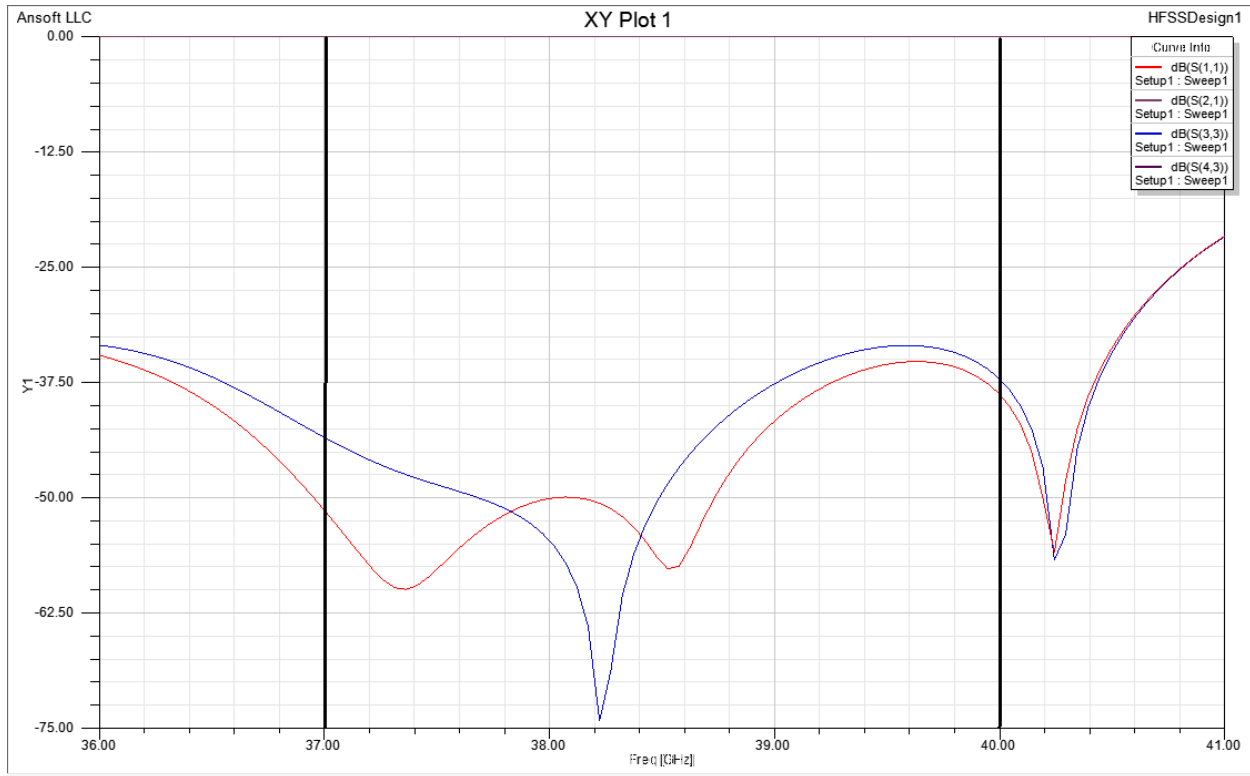
Figure 5-5 S-Parameters for Four H-Plane bends in Groove Gap waveguide

5.4 Milling Problems

As the gap waveguide requires milling of certain dimension, it always comes to challenge for mechanical engineers to fit in the dimensions. The smallest milling tool available at manufacturing facility is 0.4mm. If we recall our coupler design, we can see that at the indentations, the distance is little smaller than 0.4mm. Also the central pins at indentations are quite small, thus will not be able to withstand mechanical stress. Therefore, the indentation was slight moved to provide exactly 0.4mm distance among the pins. Also the central indentation pin was made thicker by extending it in one direction. Thus it provided the necessary rigidity to the pin. As a result of these changes, a little degradation is noticed. Slight increase in the amplitude difference and reflection coefficients is the result of these changes. In Figure 5-6, final mechanical layout and results are shown.
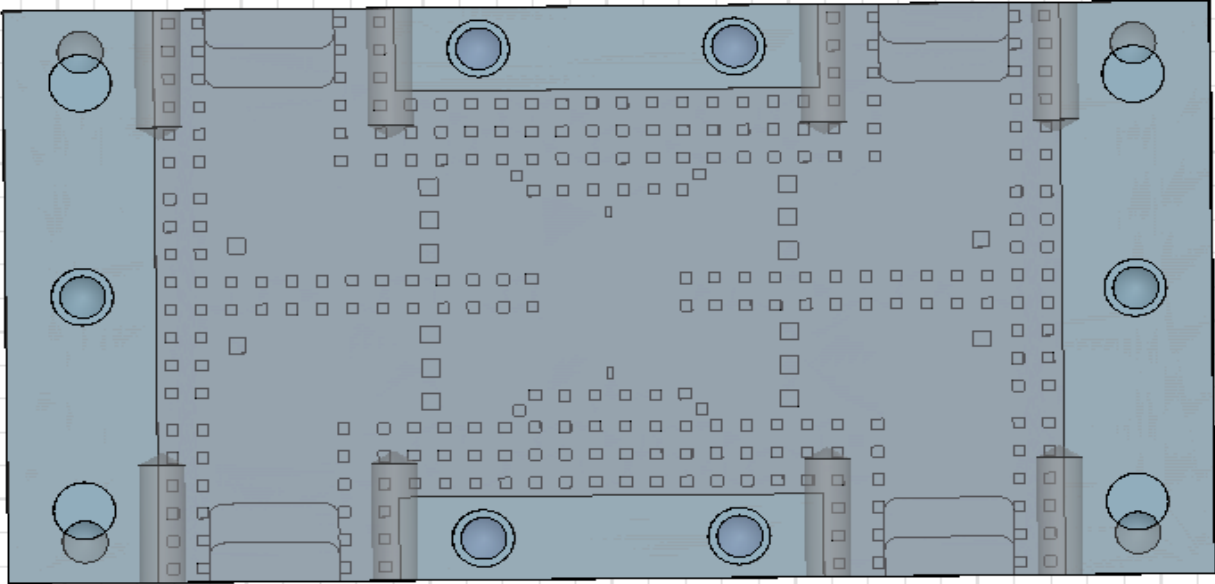
(a)
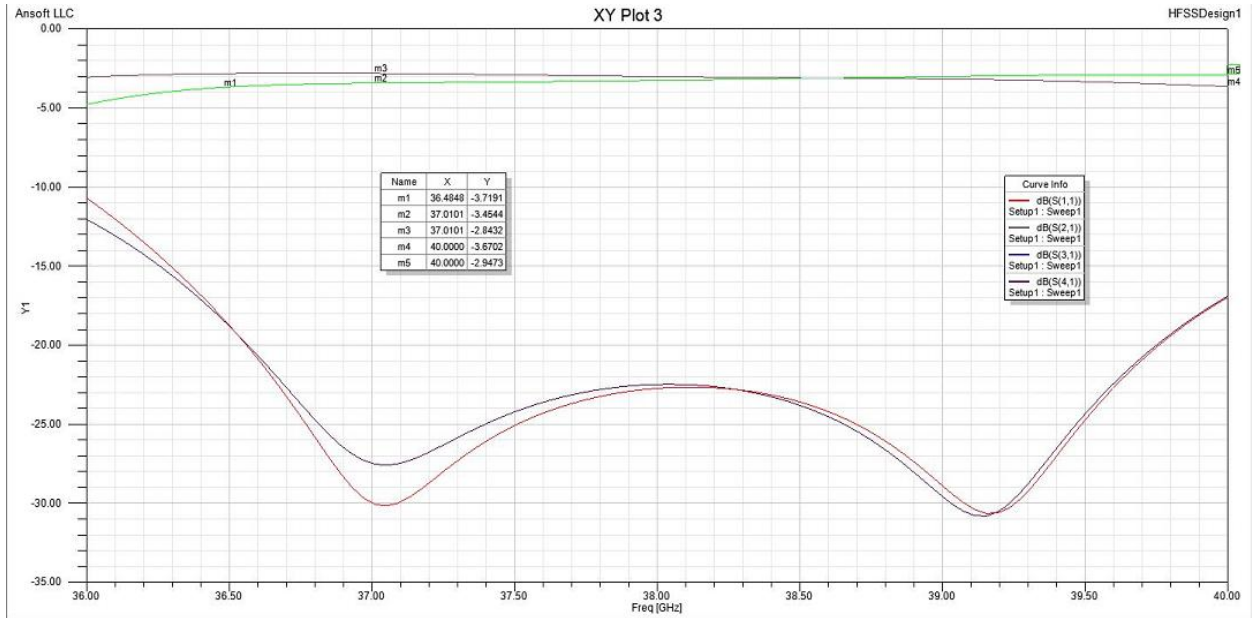
(b)

Figure 5-6 a) Final Mechanical Layout of Coupler in Groove Gap waveguide. b) S-Parameters for Finalized Structure

6 Chapter 6

6.1 Measurements and Conclusions

This chapter contains the measurement results and the conclusions drawn from those measurements. All the measurements were performed at Antenna department, Chalmers University of Technology. For measurements, we have used standard WR 28 calibration kit with Vector Network Analyzer (). For plotting and comparison, matlab was used as a plotting platform. Matlab codes can be accessed in appendix.

6.2 Calibration of VNA

Before performing the measurements, VNA was calibrated using TRL calibration. For this calibration, standard calibration kit for WR 28 rectangular waveguide was used. After the calibration, it was noted that return loss was less than -40dB for

standard through transmission. Moreover, the frequency range selected for measurement was 30-40GHz. As it is mentioned before that our designed gap waveguide works in the range of 30-43 GHz.

6.3   Measurements

As we have to measure a four port device using a two port VNA. We have used two WR28 loads, in order to terminate the two remaining ports. These loads were tested and have shown a return loss of -40dB over the entire frequency range. We have taken measurements with different combinations of terminating and transmitting ports. The measured S parameters for our hybrid coupler is shown in Figure 6-1
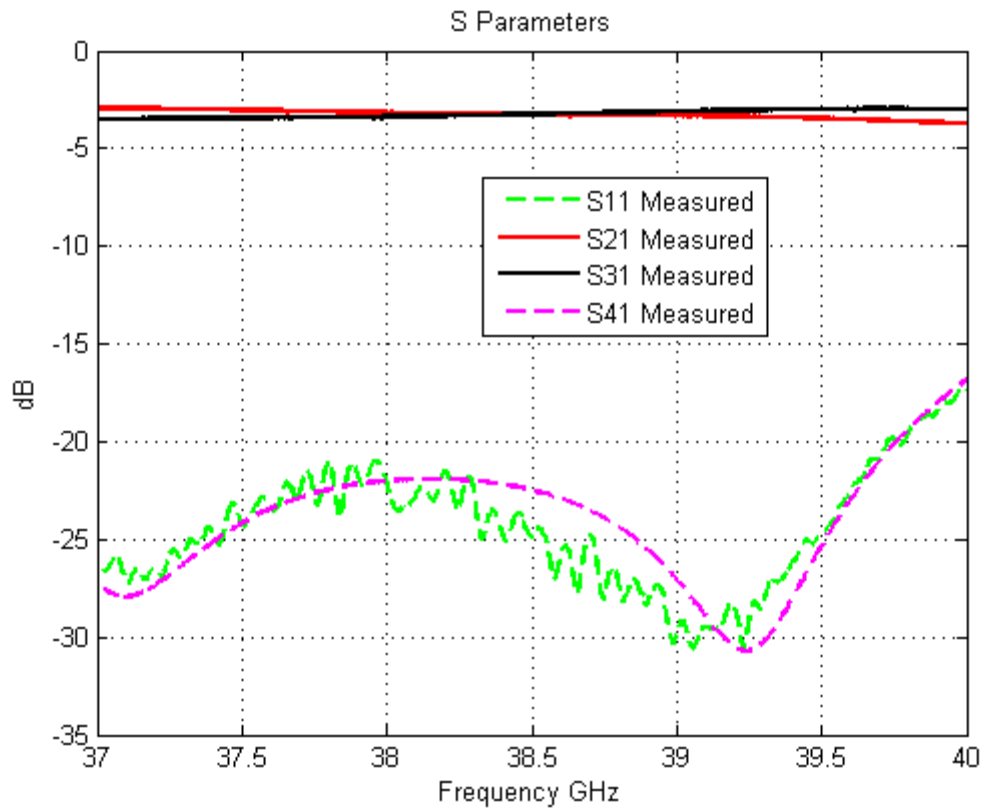
Figure 6-1 Measured S-Parameters for Coupler in groove waveguide

We can see from the results that the measured and simulated parameters are in agreement. Hence it can be safely said that the hybrid coupler we have designed,

can work in the range of 37-40 GHz. A more detailed analysis of these measurements was made in the coming sections.

6.4 Analysis

Analysis of results can be divided into following categories.

- Amplitude Analysis

- Phase Analysis

- Wide Band Analysis

The measurements are analyzed over the range of 37-40 GHz; it is our desired frequency range as mentioned in chapter 1. Finally a wide band analysis is performed in order to estimate the percentage bandwidth of the this hybrid coupler.

6.4.1 Amplitude Analysis

To compare simulated and measured results, S parameters of simulations were imported using HFSS export utility in matlab. Then a difference of simulated and measured results was plotted over the frequency range. These plots are shown in figure 6-2.
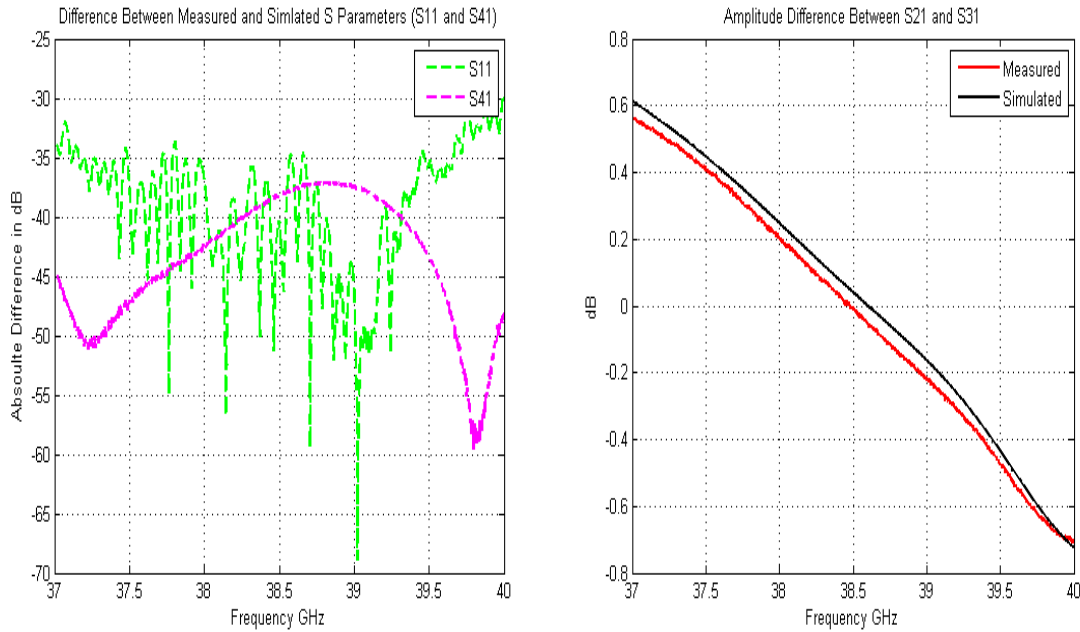
Figure 6-2 Amplitude Difference between Measure and Simulated Results

From figure 6-2 as we can see that the amplitude difference between measured and simulated values is in the range of ±0.04dB. Amplitude difference is calculated by subtracting S21 and S31 (both in dB for measure and simulated results). S11 shows a rippled plot. The reason is that calibration of short in TRL was not performed accurately, therefore the response in not smooth for S11. Therefore, we have plotted an absolute difference between measured and simulated results. The absolute difference is calculated by subtracting the S-parameters (measured and simulated) and then taking the absolute value for this complex difference, finally the values are expressed in dB. We can see that for S11 and S41 the absolute difference is some what below -30dB. By this analysis, we can safely say that the amplitude of all S parameters meet the design requirements. Although the return loss for 40GHz is a little high, yet it was the same in simulation results.

6.4.2 Phase Analysis

The exact phase of S21 and S31 is not easy to determine from Measured S parameters, As it involves the complex phase unwrapping algorithms. But we can find the phase difference of coupled and though port. As the measurements were

complex S parameters, a plot was obtained for the phase difference of through and coupled port. This plot is shown in figure 6-3
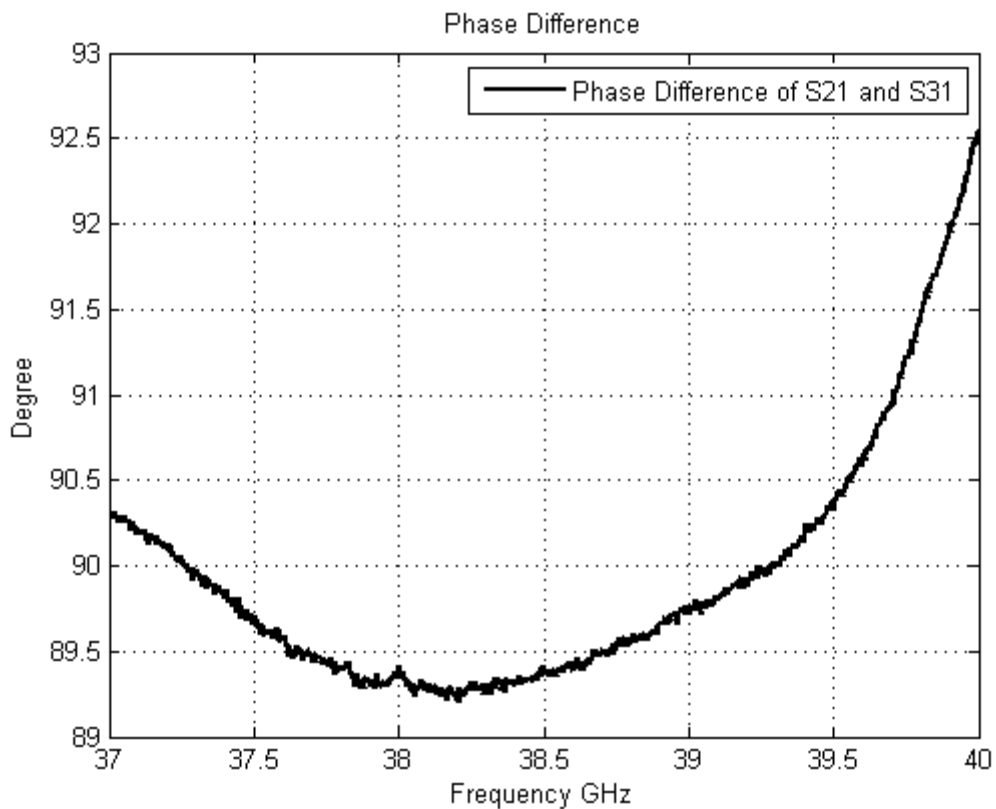
Figure 6-3 Phase Difference between Coupled and through port

As can be seen from the above figure that the phase difference over the entire frequency range is $90°$ with a difference of $±2.5°$. Therefore, we can safely say that our designed coupler is a $90°$ hybrid coupler.

6.4.3 Wide Band Analysis

So far we have analyzed the results in our designed frequency range. But we can observe from figure 6-1 that the coupler can work in a wider range. Therefore, in order to estimate the total bandwidth of coupler, a plot was obtained with extended frequency range, as shown in figure 6-4.
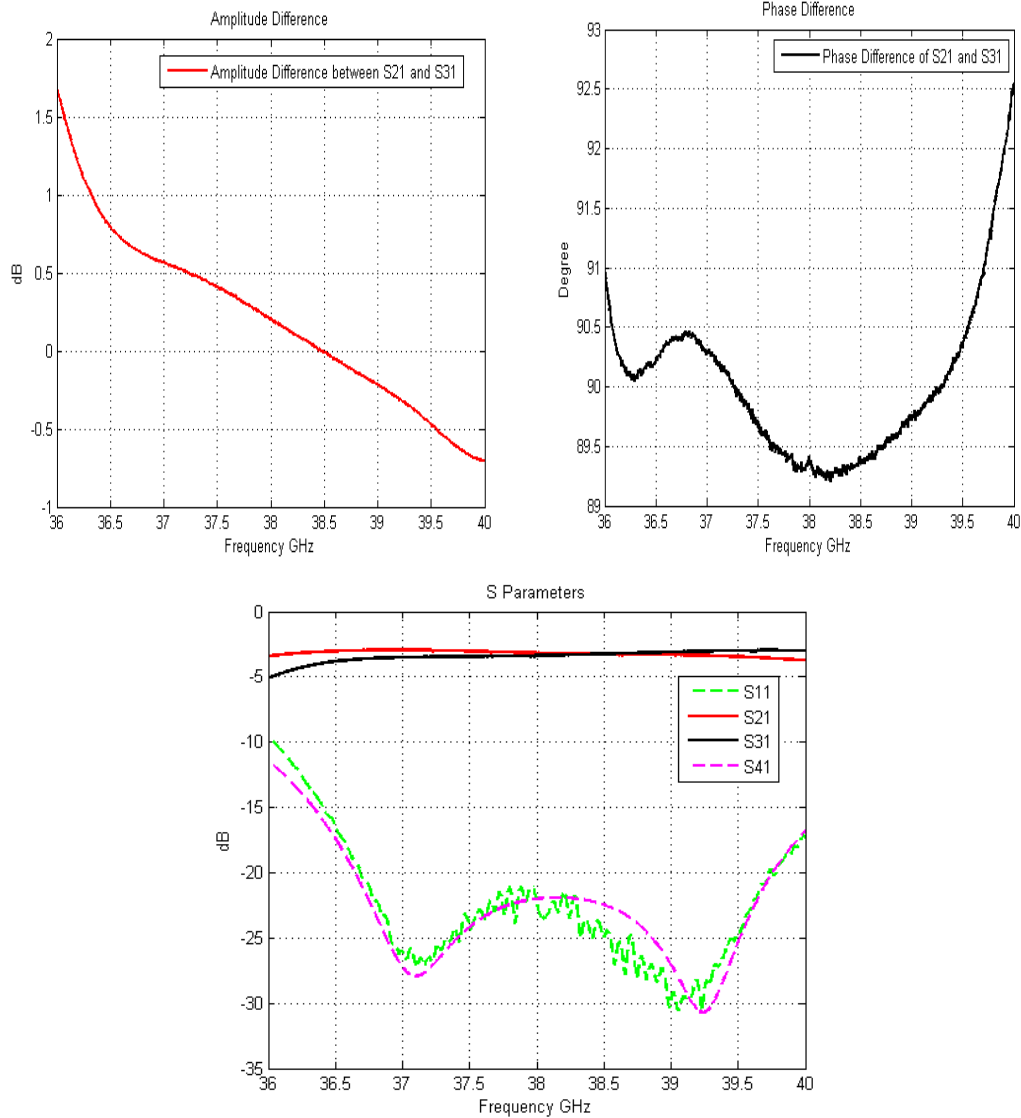
Figure 6-4 Wide-band S-Parameters for Hybrid Groove waveguide coupler

From figure 6-4, we can see that our coupler is working from 36.5GHz to 40GHz. This makes 9.1% bandwidth with a return loss of -17dB and an amplitude difference of 0.7dB. We can safely say that with a more optimized design it is also possible to get a 10% bandwidth with same electrical performance.

6.5 Conclusions

After a detailed analysis of measurements, it is proven that groove gap waveguide is fully capable of replacing conventional hollow waveguide technology. Being a

planar technology, it can easily be designed and optimized for different components and frequency ranges. This report also establishes the fact that Gap waveguides are fully compatible with conventional waveguides and same measurement methods can be used. If we look at the design closely, we can easily observe that it requires a large milling time and thus increases the manufacturing costs. But on the other hand, it's a planar technology; therefore it can be casted using casting techniques for metal structures.

Finally we can conclude that Gap waveguide is a promising technology and a good alternative for Terahertz applications. It has the potential to change today's microwave industry. Efforts are needed to integrate this technology with active components. It requires new software techniques as well as new interface challenges. It is anticipated that more research work will be put in this thrilling novelistic approach and soon a terahertz device will be designed.

7 References

[1] A. Valero-Nogueira, E. Rajo-Iglesias, P.-S. Kildal, E. Alfonso, "Local metamaterial-based waveguides in gaps between parallel Metal Plates", IEEE Antennas and Wire-less Propagation letters (AWPL), Vol. 19, pp. 84-7, 2009

[2] J. R. Costa, M. G. Silveirinha, C. A. Fernandes, "Electromagnetic characterization of textured surfaces formed by metallic pins", IEEE Trans. Antennas Propag., Vol. 56, pp. 405-15, 2008.

[3] P.-S. Kildal and A. Kishk, "EM modelling of surfaces with stop or go characteristics-artificial magnetic conductors and soft and hard surfaces". App. Comput. Electro-magn. Soc. J., Vol.18, pp.32-34, March 2003.

[4] P.-S. Kildal, "Three metamaterial-based gap waveguides between parallel metal plates for mm and submm waves", in 2009 3rd European Conference on Antennas and Propagation. EuCAP 2009, 23-27 March 2009, Piscataway, NJ, USA, 2009, pp. 28-32

[5] Per-Simon Kildal, "Foundation of antennas, a unified approach Compandium in Antenna Engineering", Chalmers University of Technology Sweden ,2009.

[6] Jens Bornemann Jarosla Uher, "Waveguide components for antenna feed systems" Theory and Cad, Addison Wesley, 1976.

[7] P.-S Kildal, "Definition of artificially soft and hard surfaces for electromagnetic waves" Electron. Lett.,Vol.24, pp.168-170, 1998.

[8] Romulo F, Jimenez Broas Nicholas G, Alexopolous Dan Sievenpiper, Lijun Zhang and Eli Yablonovitch, "High-impedance electromagnetic surfaces with a forbidden frequency band", IEEE transcations on Microwave Theory and Techniques, Vol. 47, pp.1-2, 1999.

[9] P.-S. Kildal, Eva, Rajo-Iglesias, "Cut-off bandwidth of metamaterial-based parallel-plate gap waveguide with one textured metal pin surface", 3rd European Conf, Antennas Propagat. (EuCAP 2009), Berlin, Germany, Vol.:23-27, March 2009.

[10] E. Rajo-Iglesias, M. Caiazzo, L.Inclan, P.S Kildal, "Comparison of bandgaps of mashroom-type EBG surface, corrugated and strip-type soft surfaces", IET Microw,Antenna Propag, Vol. 1, pp.1-2, Feb 2007.

[11] E. Rajo-Iglesias, Ashraf Uz Zaman, P.S Kildal, "Parallel plate cavity mode suppression in microstrip circuit packages using a lid of nails", IEEE Microwave and Wireless Components Letters, Vol. 20, pp.1-2, Jan 2010.

[12] Z.Sipus, H.Merkel, P.S Kildal, "Green's function for planar soft and hard surfaces derived by asymptotic boundary conditions". IEEE Proc. Part H, Vol. 47, pp.1-2, Oct. 1997.

[13] Rajo-Iglesias, P.-S Kildal,"Groove gap waveguide: A rectangular waveguide between contactless metal plates enabled by parallel-plate cut-off" in 4th European Conference on Antennas and Propagation (EucCAP 2010), 12-16 April 2010, Piscataway, NJ, USA, 2010,

[14] H.J.Riblet," A mathematical theory of Directional Coupler", I.R.E Proc, Vol.33, pp.1307-1313), 1947

[15] H.J.Riblet, "Short-Slot Hybrid Junction", I.R.E Proc,Vol.34, pp.1307-1313, 1947

[16] Zhewang Ma, Taku Yamane, Eikichi Yamashita, "Analysis and design of H-Plane waveguide bends with compact size, wideband and low return loss characteristics". University of Electro-Communication, Chofu-Shi Tokyo, Japan.

[17] David M.Pozar. Microwave Engineering 3rd edition. Wiley

[18] Robert E. Collins.Foundation of Microwave Engineering 3rd edition. Wiley

[19] http://www.wikipedia.com

8 Appendix

```matlab
s11=zeros(961,1);
s21=zeros(961,1);
s31=zeros(961,1);
s41=zeros(961,1);
freq=zeros(961,1);
for i=1:961
    freq(i,1)=S21(i,1)*10^-9;
    s11(i,1)=S21(i,2)+1i*(S21(i,3));

    s21(i,1)=S21(i,4)+1i*S21(i,5);

    s31(i,1)=S31(i,4)+1i*S31(i,5);

    s41(i,1)=S41(i,4)+1i*S41(i,5);

end
mag_s11=zeros(961,1);
mag_s21=zeros(961,1);
mag_s31=zeros(961,1);
mag_s41=zeros(961,1);
ang_s21=zeros(961,1);
ang_s31=zeros(961,1);
for i=1:961
    mag_s11(i,1)=abs(s11(i,1));
    mag_s21(i,1)=abs(s21(i,1));
    mag_s31(i,1)=abs(s31(i,1));
    mag_s41(i,1)=abs(s41(i,1));
    ang_s21(i,1)=angle(s21(i,1));
    ang_s31(i,1)=angle(s31(i,1));
end
%  for i=1:961
%     mag_s11(i,1)=abs(s11(i,1));
%     mag_s21(i,1)=abs(s21(i,1));
%     mag_s31(i,1)=abs(s31(i,1));
%     mag_s41(i,1)=abs(s41(i,1));
% end

sim_s11=zeros(961,1);
sim_s21=zeros(961,1);
sim_s31=zeros(961,1);
sim_s41=zeros(961,1);
sim_freq=zeros(961,1);
for i=1:961
    sim_freq(i,1)=(sim_s(i,1))*exp(9);
    sim_s11(i,1)=sim_s(i,4)+1i*(sim_s(i,3));
    sim_s21(i,1)=sim_s(i,7)+1i*(sim_s(i,6));
    sim_s31(i,1)=sim_s(i,10)+1i*(sim_s(i,9));
    sim_s41(i,1)=sim_s(i,13)+1i*(sim_s(i,12));

end
```

```matlab
figure(1)
plot(freq,(20*log10(mag_s11)), 'g--', 'linewidth',2);hold on
plot(freq,(20*log10(mag_s21)), 'r-', 'linewidth',2);hold on
plot(freq,(20*log10(mag_s31)), 'k-', 'linewidth',2);hold on
plot(freq,(20*log10(mag_s41)), 'm--', 'linewidth',2);
% plot(freq,20*log10(abs(sim_s11)), 'm--', 'linewidth',1);hold on
% plot(freq,20*log10(abs(sim_s21)), 'g--', 'linewidth',1);hold on
% plot(freq,20*log10(abs(sim_s31)), 'y--', 'linewidth',1);hold on
% plot(freq,20*log10(abs(sim_s41)), 'k--', 'linewidth',1);

grid on
legend('S11 Measured','S21 Measured','S31 Measured','S41 Measured','simulated
S11','simulated S21','simulated S31','simulated S41')
xlabel('Frequency GHz')
ylabel('dB')
title('S Parameters')
axis auto
figure(2)
plot(freq,20*log10(abs(s11-sim_s11)), 'g--', 'linewidth',2);hold on
% plot(freq,20*log10(1+(abs(s21-sim_s21))), 'r-', 'linewidth',2);hold on
% plot(freq,20*log10(1+(abs(s31-sim_s31))), 'k-', 'linewidth',2);hold on
plot(freq,20*log10(abs(s41-sim_s41)), 'm--', 'linewidth',2);
% plot(freq,(sim_s11), 'm--', 'linewidth',1);hold on
% % plot(freq,(sim_s21), 'g--', 'linewidth',1);hold on
% % plot(freq,(sim_s31), 'y--', 'linewidth',1);hold on
% plot(freq,(sim_s41), 'k--', 'linewidth',1);

grid on
legend('S11','S41')
xlabel('Frequency GHz')
ylabel('Absoulte Difference in dB')
title('Difference Between Measured and Simlated S Parameters (S11 and S41)')
axis auto
figure (3)
plot(freq,(mod((ang_s21-ang_s31),2*pi))*180/pi, 'k-', 'linewidth',2);hold on
grid on
legend('Phase Difference of S21 and S31')
xlabel('Frequency GHz')
ylabel('Degree')
title('Phase Difference')
axis auto
figure (4)
plot(freq,(20*log10(mag_s21))-(20*log10(mag_s31)), 'r-', 'linewidth',2);hold
on
plot(freq,20*log10(sim_s21)-20*log10(sim_s31), 'k-', 'linewidth',2);
grid on
legend('Measured','Simulated')
xlabel('Frequency GHz')
ylabel('dB')
title('Amplitude Difference Between S21 and S31')
axis auto
```